

# Essentiality of the Non-stoquastic Hamiltonians and Driver Graph Design in Quantum Optimization Annealing

Vicky Choi  
Gladiolus Veritatis Consulting Co.

June 7, 2022

## Abstract

One of the distinct features of quantum mechanics is that the probability amplitude can have both positive and negative signs, which has no classical counterpart as the classical probability must be positive. Consequently, one possible way to achieve quantum speedup is to explicitly harness this feature. Unlike a stoquastic Hamiltonian whose ground state has only positive amplitudes (with respect to the computational basis), a non-stoquastic Hamiltonian can be *eventually stoquastic* or *properly non-stoquastic* when its ground state has both positive and negative amplitudes. In this paper, we describe that, for some hard instances which are characterized by the presence of an anti-crossing (AC) in a stoquastic quantum annealing (QA) algorithm, how to design an appropriate XX-driver graph (without knowing the prior problem structure) with an appropriate XX-coupler strength such that the resulting non-stoquastic QA algorithm is *proper-non-stoquastic* with two bridged anti-crossings (a double-AC) where the spectral gap between the first and second level is large enough such that the system can be operated *adiabatically* in polynomial time. The speedup is exponential in the original AC-distance, which can be sub-exponential or exponential in the system size, over the stoquastic QA algorithm, and possibly the same order of speedup over the state-of-the-art classical algorithms in optimization. This work is developed based on the novel characterizations of a modified and generalized parametrization definition of an anti-crossing in the context of quantum optimization annealing introduced in [4].

## 1 Introduction

Adiabatic quantum computation in the quantum annealing form is a quantum computation model proposed for solving the NP-hard combinatorial optimization problems, see [1] for the history survey and references therein. A quantum annealing algorithm is described by a system Hamiltonian

$$\mathcal{H}(s) = (1 - s)\mathcal{H}_{\text{driver}} + s\mathcal{H}_{\text{problem}} \quad (1)$$

where the driver Hamiltonian  $\mathcal{H}_{\text{driver}}$ , whose ground state is known and easy to prepare; the problem Hamiltonian  $\mathcal{H}_{\text{problem}}$ , whose ground state encodes the solution to the optimization problem;  $s \in [0, 1]$  is a parameter that depends on time. A typical example of the system Hamiltonian is the transverse-field Ising model where the driver Hamiltonian is  $\mathcal{H}_X = -\sum_{i \in \mathcal{V}(G)} \sigma_i^x$ , and the problem Hamiltonian  $\mathcal{H}_{\text{problem}}$  is an Ising Hamiltonian:  $\mathcal{H}_{\text{Ising}} = \sum_{i \in \mathcal{V}(G)} h_i \sigma_i^z + \sum_{ij \in \mathcal{E}(G)} J_{ij} \sigma_i^z \sigma_j^z$  defined on a problem graph  $G = (\mathcal{V}(G), \mathcal{E}(G))$ , which encodes the optimization problem to be solved. The quantum processor that implements the many-body system Hamiltonian is also referred to as a *quantum annealer* (QA). The QA system is initially prepared in the known ground state of  $\mathcal{H}_{\text{driver}}$ , and then through a quantum evolution process, it reaches the ground state of  $\mathcal{H}_{\text{problem}}$  at the end

of the evolution. We will consider the driver Hamiltonian  $\mathcal{H}_{\text{driver}}$  that includes both X-driver term:  $\mathcal{H}_X = -\sum_{i \in V(G)} \sigma_i^x$ , and XX-driver term  $\mathcal{H}_{XX} = J_{xx} \sum_{ij \in E(G_{\text{driver}})} \sigma_i^x \sigma_j^x$  where  $G_{\text{driver}}$  is the driver graph, and  $J_{xx}$  can be positive or negative real numbers. A Hamiltonian is originally defined to be *stoquastic* [2] if its non-zero off-diagonal matrix elements in the computational basis are all negative; otherwise, it is called *non-stoquastic*. Thus,  $\mathcal{H}_{XX}$  is stoquastic if  $J_{xx} < 0$  and non-stoquastic if  $J_{xx} > 0$ . Below, we will discuss a refinement of the non-stoquasticity. We consider the following three types of driver Hamiltonians:

$$\mathcal{H}_{\text{driver}} = \begin{cases} \mathcal{H}_X & (D1) \\ \mathcal{H}_X + \mathcal{H}_{XX} & (D2) \\ \mathcal{H}_X + s\mathcal{H}_{XX} & (D3) \end{cases}$$

Type (D1) is the standard transverse field driver Hamiltonian with the uniform superposition state as the (initial) ground state. At this point it is unclear what kind of (D2) Hamiltonian is possible to prepare experimentally, even if the (initial) ground state is known. For this reason, we consider the type (D3) driver Hamiltonian, which is known as the catalyst [3], with the uniform superposition state as the (initial) ground state. In this paper, we consider the NP-hard MWIS problem (which any Ising problem can be easily reduced to [4]). We will denote the system Hamiltonian in Eq. (1) for solving the WMIS problem on the weighted  $G$  by  $\text{SysH}(\mathcal{H}_X, G)$  when  $\mathcal{H}_{\text{driver}} = \mathcal{H}_X$ ; and by  $\text{SysH}(J_{xx}, G_{\text{driver}}, G)$  when  $\mathcal{H}_{\text{driver}} = \mathcal{H}_X + s\mathcal{H}_{XX} = \mathcal{H}_X + s(J_{xx} \sum_{ij \in E(G_{\text{driver}})} \sigma_i^x \sigma_j^x)$ , without explicitly stating the weight function  $w$  on  $G$ .

Typically, QA is assumed to be operated adiabatically, and the system remains in its instantaneous ground state throughout the entire evolution process. However, QA can be operated non-adiabatically when the system undergoes diabatic transitions to the excited states and then return to the ground state. The former is referred to as AQA, and the latter as DQA. Recently, some quantum enhancement with DQA were discussed in [5]. It is worthwhile to point out that the DQA defined there means that the system remains in a subspace spanned by a band of eigenstates of the system Hamiltonian and it does not necessarily return to the ground state at the end of the evolution. We are interested in successfully solving the optimization problem and therefore require the system returns to the ground state. To distinguish these two versions, we shall refer to our version of DQA as DQA-GS. DQA-GS has been exploited for the possible quantum speedup by an oracular stoquastic QA algorithm in [6, 7]. More discussion on this in Section 3.

The running time of a QA algorithm is the total evolution time,  $t_f = s^{-1}(1)$ . According to the Adiabatic Theorem (see, e.g., [9] for a rigorous statement), the run time of an AQA algorithm is inversely proportional to a low power of the minimum spectral gap (min-gap),  $\Delta_{10}(s^*) = \min_s E_1(s) - E_0(s)$ , where  $E_0(s)$  ( $E_1(s)$ , resp.) is the energy value of the ground state (the first excited state, resp.) of  $\mathcal{H}(s)$ . Thus far, the possible quantum speedup of the transverse-field Ising-based QA as a heuristic solver for optimization problem over state-of-the-art classical (heuristic) algorithms has been called into questions, see [5] for a discussion. As a matter of fact, the min-gap can be exponentially small in the problem size and thus an AQA algorithm can take an exponential time, without achieving a quantum advantage. Indeed, one can easily construct instances that have an exponentially small gap due to an anti-crossing between levels corresponding to local and global minima of the optimization function, see e.g., [4, 10].

Anti-crossing (AC), also known as avoided level crossing or level repulsion, is a well-known concept for physicists. In the context of adiabatic quantum optimization (AQO), the small-gap due to an anti-crossing has been explained in terms of some established physics theory, such as first-order phase transition [10], Anderson localization [11]<sup>1</sup>. In these two cases, the argument was based on applying the perturbation theory at the end of evolution where the anti-crossing occurs. Such an anti-crossing was later referred to as a perturbative crossing,

---

<sup>1</sup>A correction to the paper in [12].

see e.g. [3]. A parametrization definition of an anti-crossing was first introduced by Wilkinson in [13], and was used in [14] to study the effect of noise on the QA system. In [4], we gave a parametrization definition for an anti-crossing in the context of quantum optimization annealing where we also describe the behavior of the energy states that are involved in the anti-crossing, including the symmetry-and-anti-symmetry (SAS) property of the two states at the anti-crossing point.

In this paper, we modify and generalize the parametrization definition of the anti-crossing in [4]. We derive some novel characteristics of such an anti-crossing and develop it into an analytical tool for the design and analysis of the QA algorithm. In particular, (1) we discover the significance of the sign of the coefficients of the states involved in the anti-crossing which leads to the revelation of the significant distinction between the *proper* non-stoquastic and *eventually-stoquastic* Hamiltonians (to be elaborated below). (2) We derive the AC-gap bound analytically, including the factors that affect the gap size, based on the approximate SAS property of the two states at the anti-crossing point. This then directly allows us to study how the AC-gap changes (without actually computing the gap size) as we vary one parameter in the system Hamiltonian, including either the parameters in the problem Hamiltonian or the XX-coupler strength in the driver Hamiltonian. The gap size is not only important for the run-time of the adiabatic algorithm<sup>2</sup>, but it is also crucial for the analysis of the diabatic transition in DQA setting.

We now describe our main results. We consider some hard MWIS instances which have a special structure, namely, there is a set of near-cost (or almost degenerate) local minima that are constituted by a set of disconnected components. In the MWIS case, each component is necessarily a clique (because of the maximality of the independent set). The local minima are formed from one element from each clique, thus if there are  $k$  cliques, each of size  $t$ , there will be  $t^k$  local minima. Such a set of local minima  $L$  would cause a formation of an anti-crossing in a stoquastic quantum annealing (QA) algorithm. We show if we take the edges in the cliques as the XX-couplers in the driver graph, and if the XX-coupler strength  $+J_{xx}$  is large enough, it will force  $L$  to split into two opposite subsets, namely  $L^+$  (states with positive amplitudes) and  $L^-$  (state with negative amplitudes), if  $L$  is to occupy the instantaneous ground state (while its energy is minimized). This in turn will result in two anti-crossings bridged by  $(L^+, L^-)$ , called a *double-AC*. That is, if we take  $G_{\text{driver}} = G|_L$ , the induced subgraph in  $L$ , there is an appropriate XX-coupling strength such that the resulting non-stoquastic QA algorithm is proper-non-stoquastic with a double-AC. Consequently, if the second-level gap between the two anti-crossings is large enough, the system can be operated diabatically in polynomial time, i.e. solve the problem through DQA-GS in polynomial time. More specifically, the system diabatically transitions to the first excited state at the first AC; then it adiabatically follows the first excited state and does not transition to the second excited state because of the large second-level gap; finally, the system returns to the ground state through the second AC. The above idea can be generalized to the system that has a sequence of *nested double-ACs* or a double *multi-level anti-crossings* through *diabatic cascades* [8]. In which case, the system diabatically transitions to a band of excited states through a cascade of first ACs (of the nested double-ACs), with the condition that the band of eigenstates is well separated from the next excited state (so that the system will not transition further), and return to the ground state through a cascade of second ACs (of the nested double-ACs). The procedure of how to identify the independent cliques efficiently (as the driver graph) and how to identify the appropriate  $J_{xx}$  coupler strength is described in our algorithm DIC-DAC-DOA<sup>3</sup> in Section 2.2 when we do not have the prior knowledge of the problem structure.

<sup>2</sup>One word of caution: because of our two-level assumption (that other levels are far apart) in the AC definition, the presence of an AC implies a small gap; however, the absence of an AC does not necessarily imply a large (polynomial in the system size) gap. That is, AC-min-gap is necessarily small, but non-AC min-gap is not necessarily large.

<sup>3</sup>Stands for: Driver graph from Independent-Cliques; Double Anti-Crossing; Diabatic quantum Optimization Annealing

## 1.1 Non-stoquasticity: Eventually Stoquastic vs Proper Non-stoquastic

The distinction of the stoquasticity is vital in quantum simulations because of the ‘sign’ problem, see e.g., [15, 16] and the references therein. In particular, in [15], Hen introduced the VGP to further classify the stoquasticity of the Hamiltonian. The concept of stoquasticity is also important from a computational complexity-theory viewpoint, see [17] for the summary.

From the algorithmic design perspective, we distinguish the stoquasticity of the Hamiltonian based on the Perron-Frobenius (PF) Theorem<sup>4</sup> which we recast in our terminology.

**Theorem 1.1.** (*Perron-Frobenius Theorem*) *If a real Hermitian Hamiltonian  $A$  is non-negative (all entries are non-negative), then the ground state of  $-A$  is a non-negative vector (all entries are non-negative).*

We say  $A$  has the PF property if the ground state of  $-A$  is a non-negative vector. It has been shown that there are more general matrices that have the PF property [20, 21]. In particular,  $A$  has the PF property if  $A$  is *eventually* non-negative, i.e., there exists  $k_0 > 0$  such that  $A^k \geq 0$  for all  $k > k_0$ . In particular, the non-stoquastic  $\mathcal{H}_{XX}$  with small positive  $J_{xx}$  can have the PF property.

**Definition 1.2.** *A non-stoquastic  $\mathcal{H}$  is called proper if it fails to have the PF property (that is, the ground state has both positive and negative entries), otherwise is called eventually stoquastic.*

We shall denote the proper non-stoquastic (eventually stoquastic, stoquastic, resp.) by **PNStoq** (**EStoq**, **Stoq**, resp.). A  $\text{SysH}(J_{xx}, G_{\text{driver}}, G)$  is **EStoq**, if for all  $s \in [0, 1]$ , the corresponding  $\mathcal{H}(s)$  is **EStoq**; otherwise, i.e. if exists  $s \in [0, 1]$  such that the corresponding  $\mathcal{H}(s)$  is **PNStoq**, the  $\text{SysH}(J_{xx}, G_{\text{driver}}, G)$  is **PNStoq**. See Figure 1 for the stoquasticity of  $\text{SysH}(J_{xx}, G_{\text{driver}}, G)$ .

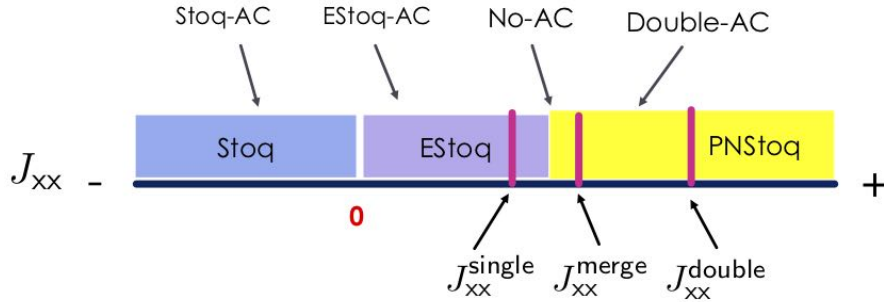


Figure 1: Stoquasticity of  $\text{SysH}(J_{xx}, G_{\text{driver}}, G)$  where  $\mathcal{H}_{XX} = J_{xx} \sum_{ij \in E(G_{\text{driver}})} \sigma_i^x \sigma_j^x$ .  $\text{SysH}(J_{xx}, G_{\text{driver}}, G)$  is **Stoq** (in blue) if  $J_{xx} < 0$ ; it is **EStoq** (in purple) if  $0 < J_{xx} < J_{xx}^{\text{transition}}$ ; and it is **PNStoq** (in yellow) if  $J_{xx} \geq J_{xx}^{\text{transition}}$ . For  $\text{SysH}(J_{xx}, G_{\text{driver}}, G)$  described in Section 2.2, the system has a double-AC when  $J_{xx} \in (J_{xx}^{\text{merge}}, J_{xx}^{\text{double}}]$  where  $J_{xx}^{\text{merge}} \geq J_{xx}^{\text{transition}}$ . As  $J_{xx}$  decreases from  $J_{xx}^{\text{double}}$ , the bridge between the two ACs shrinks, and the two ACs eventually merges, resulting in no AC, at  $J_{xx}^{\text{merge}}$ . However, no AC does not necessarily imply that the gap is not small. Also, the strength of EStoq-AC (or Hxx-Stoq-AC) increases as  $J_{xx}$  decreases:  $\text{AC-Gap}(\text{EStoq-AC}) < \text{AC-Gap}(\text{Hx-AC}) < \text{AC-Gap}(\text{Hxx-Stoq-AC})$ .

Recently, it has been claimed that for ‘‘most’’ systems, the min-gap of the non-stoquastic Hamiltonian is smaller than its ‘‘de-signed’’ stoquastic counterpart [17]. However, we show by a counter-argument (in Observation 1 of Section 2.2) and a counter-example (see Figures 8 and 10) that the opposite is true when the

<sup>4</sup>This property was used by others e.g. [18, 19] in spectral gap analysis but in a different way.

non-stoquastic Hamiltonian is eventually stoquastic and an appropriate driver graph (which can be constructed efficiently) is taken into consideration. The driver graph is either not explicitly addressed or assumed to be the same as the problem graph in [17].

For the **PNSToq**, its ground state has both positive and negative amplitudes. It is this proper non-stoquasticity feature, which is exclusively quantum mechanics, that we will make use of. Furthermore, there are reasons to believe that **PNSToq** Hamiltonians (with XX-driver Hamiltonians)<sup>5</sup> are not VGP [15], and thus not QMC-simulable.

## 1.2 Preliminary and Notation

We now introduce some necessary notation. Let  $|E_k(s)\rangle$  ( $E_k(s)$  respectively) be the instantaneous eigenstate (energy respectively) of the system Hamiltonian  $\mathcal{H}(s)$  in Eq.(1) at time  $s$ , i.e.,  $\mathcal{H}(s)|E_k(s)\rangle = E_k(s)|E_k(s)\rangle$  for  $k = 0, 1, \dots$ . For convenience, we write  $E_k \stackrel{\text{def}}{=} E_k(1)$  and  $|E_k\rangle \stackrel{\text{def}}{=} |E_k(1)\rangle$  for the energy and state of the problem (final) Hamiltonian. We express the instantaneous eigenstates ( $|E_0(s)\rangle, |E_1(s)\rangle$ ) in terms of the problem eigenstates ( $|E_k\rangle$ ):

$$\begin{cases} |E_0(s)\rangle = \sum_k c_k(s)|E_k\rangle, & \sum_k |c_k(s)|^2 = 1 \\ |E_1(s)\rangle = \sum_k d_k(s)|E_k\rangle, & \sum_k |d_k(s)|^2 = 1 \end{cases}$$

That is, we have  $c_k(s) = \langle E_0(s)|E_k\rangle$  and  $d_k(s) = \langle E_1(s)|E_k\rangle$  for all  $k$ . In general (in the proper non-stoquastic case),  $c_k(s)$  can be positive or negative, and/or can change the sign during the evolution course. Since the squared overlap  $|c_k(s)|^2$  would lose the sign of  $c_k(s)$ , we introduce the signed overlap,  $\text{sign}(c_k(s))|c_k(s)|^2$ . We will visualize our results using the signed overlaps whenever the signs are significant. In particular, the evolution of the signed overlaps of  $c_k(s)$  and  $d_k(s)$  will help us understand the formation of the anti-crossings during the quantum evolution. For  $A \subset 2^{[N]}$ , we denote  $|A_0(s)\rangle = \sum_{k \in A} c_k(s)|k\rangle$  and  $|A_0(s)| = \sum_{k \in A} |c_k(s)|^2$ ; similarly for  $|A_1(s)\rangle$  and  $|A_1(s)|$  (with  $c_k(s)$  replaced by  $d_k(s)$ ). Let  $\Delta_{ij}(s) = E_i(s) - E_j(s)$  be the instantaneous spectral gap between the  $i$ th and  $j$ th energy levels.

As in [4], we define the driver-dependent neighbourhood  $\text{nbr}_{\mathcal{H}_{\text{driver}}}(|\phi\rangle) = \{|\psi\rangle : \exists i.s.t. |\psi\rangle = \text{Op}_i(|\phi\rangle), \mathcal{H}_{\text{driver}} = \sum_i \text{Op}_i\}$ . By this definition,  $\text{nbr}_{\mathcal{H}_X}$  consists of the single-bit flip neighbourhood of the state. For example,  $\text{nbr}_{\mathcal{H}_X}(|101\rangle) = \{|100\rangle, |111\rangle, |001\rangle\}$ . Define  $\text{dist}_{H_D}(\phi, \psi)$  to be the number of Ops in the minimum path between  $\phi$  and  $\psi$ . When there is no confusion, we use sets and states interchangeably. For  $L, R \subset 2^N$ , define  $\text{dist}_{H_D}(L, R) \stackrel{\text{def}}{=} \min_{l \in L, r \in R} \text{dist}_{H_D}(l, r)$ . For example,  $\text{dist}_{H_X}(L, R)$  is the minimum Hamming distance between sets in  $L$  and  $R$ .

## 2 Results

### 2.1 Anti-crossing: A Tool for Design and Analysis of QA algorithm

#### 2.1.1 New Definition of Anti-Crossing

Informally, in the context of the quantum annealing, we define an anti-crossing between two consecutive levels with the following four conditions: (1) the anti-crossing point corresponds to a local minimum in the energy spectrum between the two interacting levels; (2) within the anti-crossing interval, all other energy levels are far away from the two interacting levels; (3) there are two small sets of “non-negligible” states involved in the anti-crossing; (4) a “sharp exchange” of the non-negligible states within a small width of the anti-crossing interval.

<sup>5</sup>As Itay Hen pointed out that the system with  $-\mathcal{H}_X$  as the driver Hamiltonian is **PNSToq** but it is also VGP.

More formally, a new parametrization definition of an anti-crossing between the lowest two levels (which can be straightforwardly generalized to any two consecutive levels) during the evolution of  $\mathcal{H}(s)$  in Eq. (1) is defined as follows.

**Definition 2.1.** We say that there is an  $(L, R)$ -ANTI-CROSSING at  $s_x$  if there exists two disjoint subsets  $L$  and  $R$  ( $\subset 2^{[N]}$ ), and  $\delta > 0, \gamma > 0$  such that

(i) For  $s \in [s_x - \delta, s_x + \delta]$ ,  $\Delta_{10}(s_x) \leq \Delta_{10}(s)$ ;

(ii) For  $s \in [s_x - \delta, s_x + \delta]$ ,  $\Delta_{10}(s) \ll \Delta_{k0}(s)$ , for all  $k > 1$ ;

(iii) Within the time interval  $[s_x - \delta, s_x + \delta]$ , both  $|E_0(s)\rangle$  and  $|E_1(s)\rangle$  are mainly composed of states from  $L$  and  $R$ . More precisely, let  $\tilde{L} = L \cup n(L)$ ,  $\tilde{R} = R \cup n(R)$ , such that all the possible states  $2^{[N]} = \tilde{L} \cup \tilde{R}$ , and  $\tilde{L} \cap \tilde{R} = \emptyset$ . For  $s \in [s_x - \delta, s_x + \delta]$ ,

$$|E_i(s)\rangle = |\tilde{L}_i(s)\rangle + |\tilde{R}_i(s)\rangle \simeq |L_i(s)\rangle + |R_i(s)\rangle \quad (2)$$

where  $|L_i(s)| + |R_i(s)| \in [1 - \gamma, 1]$  and  $|n(L_i)(s)| + |n(R_i)(s)| \in [0, \gamma]$ ,  $i = 0, 1$ . (Recall:  $|A_0(s)\rangle = \sum_{k \in A} c_k(s)|k\rangle$  and  $|A_1(s)\rangle = \sum_{k \in A} d_k(s)|k\rangle$ .)

(iv) Before the anti-crossing at  $s_x^- \equiv s_x - \delta$ ,  $|E_0(s_x^-)\rangle \simeq |L_0(s_x^-)\rangle$  (or  $|L_0(s_x^-)| \geq (1 - \gamma)$ ),  $|E_1(s_x^-)\rangle \simeq |R_1(s_x^-)\rangle$ ; after the anti-crossing at  $s_x^+ \equiv s_x + \delta$ ,  $|E_0(s_x^+)\rangle \simeq |R_0(s_x^+)\rangle$ ,  $|E_1(s_x^+)\rangle \simeq |L_1(s_x^+)\rangle$ .

For convenience, we shall refer  $(L, R)$  as the two *arms* of the anti-crossing (they appear in the left and right of each energy level).

The earlier definition in [4] is a special case with  $L = \{1\}$  (corresponds to  $|\text{FS}\rangle \stackrel{\text{def}}{=} |E_1\rangle$ ), and  $R = \{0\}$  (corresponds to  $|\text{GS}\rangle \stackrel{\text{def}}{=} |E_0\rangle$ ), without explicitly requiring the SAS property within  $\epsilon$  at  $s_x$  in the definition. A figure depicting an  $(L, R)$ -ANTI-CROSSING is shown in Figure 2.

By definition, there is an exchange between the same arm of the two levels. For  $\epsilon_v > 0$ , we say the  $(L, R)$ -ANTI-CROSSING is a  $(1 - \epsilon_v)$ -full-exchange anti-crossing if

$$\begin{cases} |L_0(s_x^-)| \stackrel{\dot{=}}{\epsilon_v} |L_1(s_x^+)| \\ |R_1(s_x^-)| \stackrel{\dot{=}}{\epsilon_v} |R_0(s_x^+)| \end{cases} \quad (3)$$

where  $A \stackrel{\dot{=}}{\epsilon_v} B$  means  $|A - B| \leq \epsilon_v$ . This condition in Eq. (3) is required to derive the SAS property in (C4). In this paper, we fix a small  $\epsilon_v > 0$ , and assume an  $(L, R)$ -ANTI-CROSSING satisfies this condition when we do not mention explicitly.

We re-introduce the “negligible” sets  $n(L)$  and  $n(R)$  back to the definition for the purpose of computing the AC-Gap. The set  $n(L)$  ( $n(R)$  resp.) consists all the neighboring states of  $L$  ( $R$  resp.) with distance at most  $d_l$  ( $d_r$  resp.), i.e.,

$$\begin{cases} n(L) = \{x : \exists y \in L \text{ s.t. } \text{dist}_{H_D}(x, y) \leq d_l\} \\ n(R) = \{x : \exists y \in R \text{ s.t. } \text{dist}_{H_D}(x, y) \leq d_r\} \end{cases}$$

for some  $d_l > 0, d_r > 0$ . The coefficients of states in  $n(L), n(R)$  are “negligible” but not “vanishing”. Indeed, we shall show that that the “negligible” states are what contribute to the gap size. (Similar to the idea that it is the high-order correction terms in the perturbation formula that contribute to the perturbative-crossing gap size.)

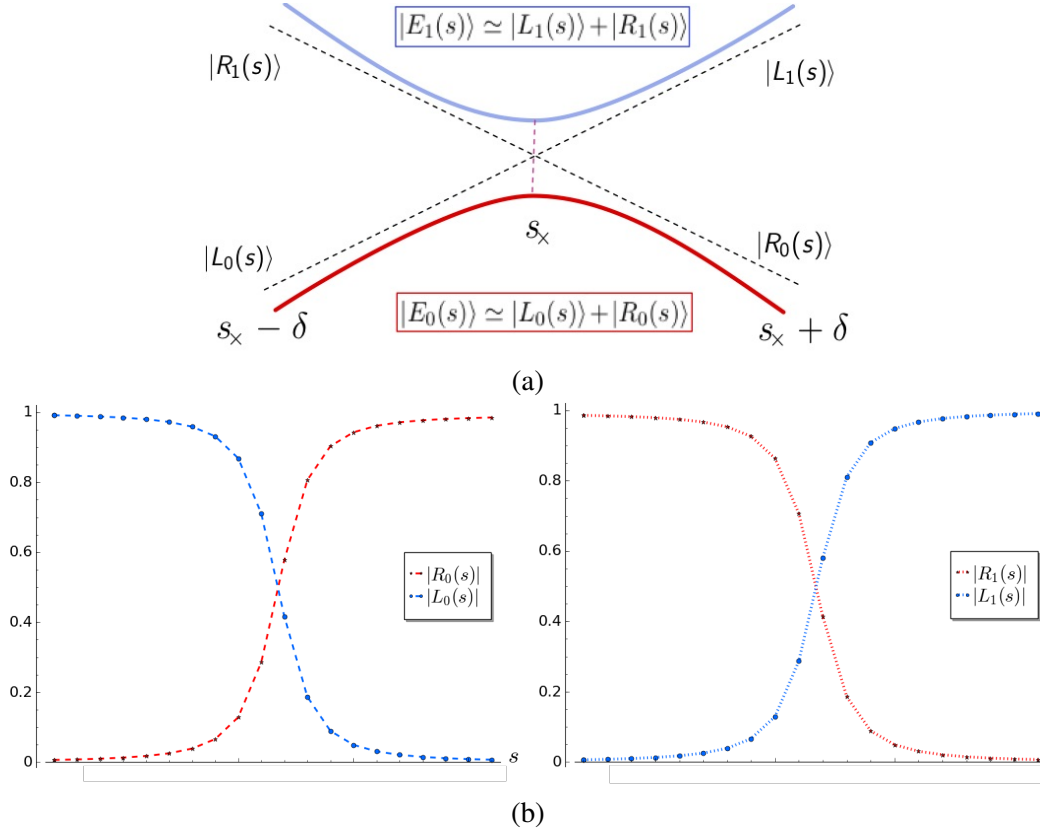


Figure 2: An  $(L, R)$ -ANTI-CROSSING at  $s_x$ . (a) Within the time interval  $[s_x - \delta, s_x + \delta]$ , both  $|E_0(s)\rangle$  and  $|E_1(s)\rangle$  are mainly composed of states from  $L$  and  $R$ . That is,  $|E_0(s)\rangle \simeq |L_0(s)\rangle + |R_0(s)\rangle$  and  $|E_1(s)\rangle \simeq |L_1(s)\rangle + |R_1(s)\rangle$  where  $|A_i(s)\rangle = \sum_{k \in A} f_k^i(s) |k\rangle$ , with  $f_k^0 = c_k, f_k^1 = d_k, A \in \{L, R\}, i = 0, 1$ . (b) When  $s$  goes from  $s_x - \delta$  to  $s_x + \delta$ , the state  $|E_0(s)\rangle$  shifts from  $L$  to  $R$  while  $|E_1(s)\rangle$  shifts from  $R$  to  $L$ :  $|L_0(s)| \downarrow, |R_0(s)| \uparrow$  while  $|R_1(s)| \downarrow, |L_1(s)| \uparrow$ , where  $|A_i(s)| = \sum_{k \in A} |f_k^i(s)|^2$  is the total magnitude in  $A_i(s)$ , for  $A \in \{L, R\}, i = 0, 1$ . The figures show the evolution of  $|L_0(s)|$  and  $|R_0(s)|$  (left) and  $|L_1(s)|$  and  $|R_1(s)|$  (right) within the interval  $[s_x - \delta, s_x + \delta]$ .

In general, we require  $\delta$  to be small, and  $\gamma$  to be near 1. Sometimes it is possible to increase  $\gamma$  by enlarging  $L$  and/or  $R$  such that  $(L^*, R^*)$ -ANTI-CROSSING is an anti-crossing with a larger  $\gamma$  (for the same  $\delta$ ), where  $L \subseteq L^*, R \subseteq R^*$ .

Around the anti-crossing,  $L_0(s_x^-)$  and  $R_0(s_x^+)$  are the “almost” ground states; while  $R_1(s_x^-)$  and  $L_1(s_x^+)$  are the “almost” first excited states. We denote their respective energy by  $\mathcal{E}_{L_0}(s_x^-)$  and  $\mathcal{E}_{R_0}(s_x^+)$ , and  $\mathcal{E}_{R_1}(s_x^-)$  and  $\mathcal{E}_{L_1}(s_x^+)$  respectively.

Let  $\overline{E}_L$  and  $\overline{E}_R$  be the average energy (w.r.t problem Hamiltonian) in  $L$  and  $R$ . Since  $|L_0(s)\rangle = \sum_{k \in L} c_k(s) |E_k\rangle$ , and if we assume  $\langle L | H_D | L \rangle = 0$ , we have  $\mathcal{E}_{L_0}(s_x^-) \approx s_x^- \overline{E}_L$ . Similarly, we have  $\mathcal{E}_{L_1}(s_x^+) \approx s_x^+ \overline{E}_L$ . Also,  $\mathcal{E}_{R_0}(s_x^+) \approx s_x^+ \overline{E}_R, \mathcal{E}_{R_1}(s_x^-) \approx s_x^- \overline{E}_R$ . In particular, it will imply that  $\overline{E}_L$  is close to  $\overline{E}_R$ , a necessary condition for the  $(L, R)$ -ANTI-CROSSING to occur.

### 2.1.2 New Characterizations of the Anti-crossing

We derive some useful characteristics of the AC based on the perturbation theory. The derivation is based on the idea that in the neighborhood of  $s_x$  the behavior of these two energy levels can be approximately computed by non-degenerate perturbation theory for the two lowest energy levels while the other energy levels are far away enough to be neglected.

**Proposition 2.2.** *An  $(L, R)$ -ANTI-CROSSING has the following four properties.*

(C1) (“Hyperbolic-like curves”) *The two energy levels form two opposite parabolas around  $s_x$ :*<sup>6</sup>

$$\begin{cases} E_1(s_x + \lambda) \doteq A\lambda^2 + B_1\lambda + E_1(s_x) \\ E_0(s_x + \lambda) \doteq -A\lambda^2 + B_0\lambda + E_0(s_x) \end{cases} \quad (4)$$

for  $\lambda \in [-\delta, \delta]$ , where  $A > 0$ , and  $B_1 \simeq B_0$ . That is, we have  $E_1(s_x + \lambda) - E_0(s_x + \lambda) \doteq 2A\lambda^2 + (B_1 - B_0)\lambda + \Delta_{10}(s_x)$ . Thus, the gap at the AC point is a local minimum of the gap spectrum.

(C2) (“States-exchange”) *When  $s$  goes from  $s_x - \delta$  to  $s_x + \delta$ , the state  $|E_0(s)\rangle$  shifts from  $L$  to  $R$  while  $|E_1(s)\rangle$  shifts from  $R$  to  $L$ :  $|c_l(s)| \downarrow$  for all  $l \in L$ ,  $|c_r(s)| \uparrow$  for all  $r \in R$ ; while  $|d_r(s)| \downarrow$  for all  $r \in R$ ,  $|d_l(s)| \uparrow$  for all  $l \in L$ , where  $\downarrow$  denotes decreasing and  $\uparrow$  denotes increasing. In particular, for  $s : s_x - \delta \rightsquigarrow s_x + \delta$ ,  $|L_0(s)| \downarrow$ ,  $|R_0(s)| \uparrow$  while  $|R_1(s)| \downarrow$ ,  $|L_1(s)| \uparrow$ .*

(C3) (“Opposite signs”) *One arm is of the same sign in the two states; the other arm is of the opposite sign in the two states. That is, it is either*

$$\begin{cases} L_0 \text{ and } L_1 \text{ in the same sign: } \text{sgn}(c_l(s))\text{sgn}(d_l(s)) = +1 \text{ for all } l \in L \\ R_0 \text{ and } R_1 \text{ in the opposite sign: } \text{sgn}(c_r(s))\text{sgn}(d_r(s)) = -1 \text{ for all } r \in R \end{cases} \quad (5)$$

or the reverse.

(C4) (“Symmetry-and-anti-symmetry(SAS) at  $s_x$  ”)

$$\begin{cases} c_l(s_x) \doteq d_l(s_x) \text{ for } l \in \tilde{L} \\ c_r(s_x) \doteq -d_r(s_x) \text{ for } r \in \tilde{R} \end{cases} \quad \text{or} \quad \begin{cases} c_l(s_x) \doteq -d_l(s_x) \text{ for } l \in \tilde{L} \\ c_r(s_x) \doteq d_r(s_x) \text{ for } r \in \tilde{R} \end{cases} \quad (6)$$

Thus, we have  $|\tilde{L}(s_x)\rangle \doteq |\tilde{L}_0(s_x)\rangle \doteq (+/-)|\tilde{L}_1(s_x)\rangle$  and  $|\tilde{R}(s_x)\rangle \doteq |\tilde{R}_0(s_x)\rangle \doteq (-/+)|\tilde{R}_1(s_x)\rangle$ , i.e.

$$(*) \begin{cases} |E_0(s_x)\rangle \doteq |\tilde{L}(s_x)\rangle + |\tilde{R}(s_x)\rangle \\ |E_1(s_x)\rangle \doteq |\tilde{L}(s_x)\rangle - |\tilde{R}(s_x)\rangle \end{cases} \quad \text{or} \quad (**) \begin{cases} |E_0(s_x)\rangle \doteq |\tilde{L}(s_x)\rangle + |\tilde{R}(s_x)\rangle \\ |E_1(s_x)\rangle \doteq -|\tilde{L}(s_x)\rangle + |\tilde{R}(s_x)\rangle \end{cases}$$

Furthermore,  $|A_i(s_x)| \in [1/2 - \eta, 1/2 + \eta]$ , for  $A \in \{L, R\}$ ,  $i = 0, 1$ , with  $0 \leq \eta < \gamma/2$ .

**AC-signature.** We refer the Property (C2) as the “AC-signature” which is more general than the Hamming weight operator  $\langle HW \rangle$  introduced in [8], to describe the “sharp exchange” between the ground state and the first excited state at the anti-crossing interval.

<sup>6</sup>Throughout this paper, for convenience, we will use the notation  $\doteq$  such that  $A \doteq B$  means  $|A - B| \leq \epsilon$  for some small error tolerance  $\epsilon > 0$ .



**Significance of the Sign.** It is worthwhile to emphasize the signs of the coefficients of the two arms in Property (C3) are critical. There are two possible cases and are depicted in Figure 3. The two anti-crossings can be connected/bridged through a common arm which is of the opposite sign (otherwise one can argue by contradiction). Thus it is necessary that the bridge consists of both positive and negative amplitudes as in proper-non-stoquastic case. Furthermore, since one arm of the AC must be in the opposite sign, if the ground state only allows the positive sign (as in the stoquastic case), the possible combinations (+/+, -/+) will be less in the stoquastic case than the possible combinations (+/+, -/-, -/+, +/-) in the non-stoquastic cases. This partially explains why one would observe more ACs in the non-stoquastic case.

### 2.1.3 AC–Gap Bound

In this section we derive the analytical AC–Gap bound for the anti-crossing that satisfies the SAS properties (for a small  $\epsilon_v$ ) and also large  $\gamma$  (such that the corresponding  $L, R$  are taking as large as possible).

**Lemma 2.3.** *Assume  $\alpha = \text{dist}_{H_D}(L, R) > 3$ .*

$$\Delta_{10}(s_x) = \Theta \left( \left| \sum_{i \in g(L), j \in g(R), \langle i | H_D | j \rangle \neq 0} c_i(s_x) c_j(s_x) \langle i | H_D | j \rangle \right| \right) \quad (7)$$

where  $g(L) = \{i \in n(L) : \exists j \in n(R) \text{ s.t. } \langle i | H_D | j \rangle \neq 0\}$ ,  $g(R) = \{j \in n(R) : \exists i \in n(L) \text{ s.t. } \langle i | H_D | j \rangle \neq 0\}$ .

That is, the non-zero contributions to the gap come from the (at least  $(\alpha/2)!$ ) states in  $g(L)$  and  $g(R)$  from the ground state. Notice that we express the AC–Gap only on the ground state (it can be also on the first excited state as  $c_k(s_x) \doteq d_k(s_x)$ ) instead of the difference between the two levels.

Next we show that the coefficients  $c_k$  decreases in geometric order of its distance from  $L, R$ , and thus the dominated terms are those in the path of the shortest distance between  $L, R$ .

**Theorem 2.4.** *Suppose that  $R$  consists of the problem ground state  $|GS\rangle$  and possibly its low-energy neighboring states (LENS), and  $L$  consists of the lowest few almost degenerate excited states and possibly their LENS. Then AC–Gap  $\Delta_{10}(s_x) = \Theta(\zeta^{\text{dist}_{H_D}(L,R)})$  where  $0 < \zeta < 1$  depends on the anti-crossing width  $\delta$ , and the energy of its left arm  $L$  at  $s_x^-, \mathcal{E}_{L_0}(s_x^-)$ , and the energy value of its right arm  $R$  at  $s_x^+, \mathcal{E}_{R_0}(s_x^+)$ .*

Remarks.

- (a) The proof actually reveals the factors that would affect the gap size. In particular, we can study the effect on the gap size (without actually computing the gap size) by analyzing how the parameters of the anti-crossing (and the parameters of the AC–Gap) evolve as we vary one parameter in the system Hamiltonian, including either the parameters in the problem Hamiltonian or the XX-coupler strength in the driver Hamiltonian. We use this argument to justify the Claim in the next section.
- (b) The AC–Gap is necessarily exponentially small (in the AC-distance), however, it is not necessarily true that every exponentially small (even in the problem size) gap corresponds to an anti-crossing defined here. For example, it is not clear if the exponential small gap example presented in [18] corresponds to our anti-crossing because they only show that there exists an excited state whose energy is close to the ground energy level and thus condition (ii) in our definition is not necessarily satisfied. A possible future work is to generalize the AC definition between one energy level and one narrow band of closely together energy levels.

## 2.2 Quantum Speedup by DIC-DAC-DOA

**MWIS Problem.** We use the NP-hard maximum-weighted independent set (MWIS) as our model problem. We make use of the MIS problem structure to construct the driver graph. As described in [4], MWIS and Ising problem can be efficiently reduced to each other. The MIS-Ising Hamiltonian is specified by a problem graph  $G$  and a weight vector  $w$  on its vertices and a  $J_{\text{penalty}}$  (In our examples in this paper, we assume  $J_{\text{penalty}} = 4$  when we omit to mention). The formulae for computing the corresponding  $\{h, J\}$  are also described in appendix.

### 2.2.1 An illustrative Example

A MIS graph with 9 weighted vertices is depicted in Figure 4. The global minimum corresponds to the maximum independent set  $\{2, 5, 8\}$  with total weight of 4.02.  $G$  has 8 local minima,  $\{\{v_1, v_2, v_3\} : v_1 \in \{0, 1\}, v_2 \in \{3, 4\}, v_3 \in \{5, 6\}\}$ , with total weights ranging from 3.70 to 3.95. This graph can be scaled to a graph of  $3n$  vertices, where the global minimum consists of  $n$  vertices, while there are  $2^n$  local minima formed by  $n$  independent-cliques.

We will compare the evolution of stoquastic  $\text{SysH}(\mathcal{H}_X, G)$  with the evolutions of  $\text{SysH}(J_{\text{xx}}, G_{\text{driver}}, G)$  for various values of  $J_{\text{xx}}$  for the weighted graph  $G$  in Figure 4. We use three metrics to compare the evolutions of the different algorithms: (1) gap-spectrum, shown in Figure 5; (2) AC-signature (total overlaps of the two arms with the ground state and the first excited state wavefunctions), shown in Figure 6; (3) Signed overlaps (of the lowest seven problem states with the ground state and the first excited state wavefunctions), shown in Figure 7.

### 2.2.2 Local Minima Subgraph and Driver Graph $G_{\text{driver}}$

**Local minima subgraph with an independent-cliques structure.** Suppose  $L$  consists of a set of local minima of the MWIS problem. Each set in  $L$  corresponds to a maximal weighted independent set. Let  $L = \{l_1, l_2, \dots, l_m\}$ . Each  $l_i$  consists of a subset of vertices in the problem graph, e.g.  $l_1 = \{0, 3, 7\}$ . Any two sets in  $L$ , say  $l_i$  and  $l_j$ , can be disjoint or share some common vertices but they must share at least one edge in the problem graph (for otherwise,  $l_i \cup l_j$  will be independent with a larger weight, contradicting to the maximality of  $l_i$  and  $l_j$ ). Furthermore, we assume the subgraph formed by sets in  $L$ , denoted by  $G|_L \stackrel{\text{def}}{=} G[\cup_{l \in L} l]$ <sup>7</sup>, consisting of a set of  $\kappa$  disconnected components. Each component is necessarily a complete subgraph or a clique  $K_{t_i}$ , where  $t_i$  is the size of  $i$ th clique, because of the maximality of the independent set. We refer to the local minima subgraph with this special structure as an *independent-cliques* structure. That is, the local minima is covered by a set of *independent cliques* where there is no edges between vertices from any two cliques. The independent-cliques condition is stronger than a *clique cover* (whose cliques may be disjoint but not necessarily independent, i.e. two cliques can be adjacent by an edge) used in the combinatorial branch-and-bound solvers for solving MIS problem [24, 25, 26]. If the weights within each clique is approximately the same, there will be  $\prod_i^{\kappa} t_i$  many almost degenerate local minima, and thus such an independent-cliques structure would cause a formation of an anti-crossing for the stoquastic QA, and would also be a main obstacle for the classical algorithms which try to enumerate all possible local minima (including the branch-and-bound algorithms).

**Claim 1.** *Suppose that  $\text{SysH}(\mathcal{H}_X, G)$  has an  $(L, R)$ -ANTI-CROSSING, where  $L$  consists of a set of local minima of the MIS problem on  $(G)$ , and  $R$  consists of the global minimum. Furthermore, we assume that the local minima subgraph has an independent-cliques structure, i.e.  $G|_L$  which consists of  $\kappa$  complete subgraphs  $K_{t_i}$  with size  $t_i$ . Let  $G_{\text{driver}} = G|_L$ . We consider  $\text{SysH}(J_{\text{xx}}, G_{\text{driver}}, G)$  for different  $J_{\text{xx}}$  while  $G_{\text{driver}}, G$  are fixed.*

<sup>7</sup>for a vertex set  $W \subset V(G)$ , its induced subgraph  $G[W]$  is defined as  $G[W] = (W, \{\{u, v\} \in E(G) : u, v \in W\})$

- (I) There exists a  $J_{\text{xx}}^{\text{single}} > 0$  such that for  $J_{\text{xx}} \in [0, J_{\text{xx}}^{\text{single}}]$ ,  $\text{SysH}(J_{\text{xx}}, G_{\text{driver}}, G)$  is eventually stoquastic, and  $\text{AC-Gap}(-J_{\text{xx}}) < \text{AC-Gap}(0) < \text{AC-Gap}(+J_{\text{xx}})$ , where  $\text{AC-Gap}(J_{\text{xx}})$  denotes the anti-crossing gap in  $\text{SysH}(G, J_{\text{xx}}, G_{\text{driver}})$ . Also, for  $J_{\text{xx}} \in [-J_{\text{xx}}^{\text{single}}, J_{\text{xx}}^{\text{single}}]$ ,  $\text{AC-Gap}(J_{\text{xx}})$  increases as  $J_{\text{xx}}$  increases.
- (II) There exist  $J_{\text{xx}}^{\text{merge}} > 0, J_{\text{xx}}^{\text{double}} > 0$  such that for  $J_{\text{xx}} \in (J_{\text{xx}}^{\text{merge}}, J_{\text{xx}}^{\text{double}}]$ ,  $\text{SysH}(J_{\text{xx}}, G_{\text{driver}}, G)$  is proper non-stoquastic and it has a double-AC bridged by  $(L^+, L^-)$ : a  $(R, L)$ -ANTI-CROSSING at  $s_1(J_{\text{xx}})$  and an  $(L, R)$ -ANTI-CROSSING at  $s_2(J_{\text{xx}})$ , where  $L^+ = \{l \in L : c_l(s) > 0\}$  and  $L^- = \{l \in L : c_l(s) < 0\} \neq \emptyset$  for  $s \in [s_1(J_{\text{xx}}), s_2(J_{\text{xx}})]$ . Furthermore, if  $1 \leq t_i \leq 2$ , for all  $i = 1, \dots, \kappa$ , then there is no AC within  $[s_1(J_{\text{xx}}), s_2(J_{\text{xx}})]$  between the first and second energy level, and there is a  $J_{\text{xx}}$  such that  $\Delta_{21}(s)$  is large, for  $s \in [s_1(J_{\text{xx}}), s_2(J_{\text{xx}})]$ .

We justify our Claim by three main observations below, supported by the numerical results of a scalable example. We leave a rigorous proof as future work. Nevertheless, our results already reveal the significance of the driver graph played in the non-stoquastic QA, and the essential difference of the **EStoq** and **PNStoq** due to different strength of  $J_{\text{xx}}$ . The evolutions of **EStoq** and **PNStoq** QAs can be very different. It is essential to distinguish them when considering non-stoquastic Hamiltonians. For example, our result in (I), where the non-stoquastic is **EStoq**, already provides a counter-example<sup>8</sup> to [17], as shown in Figure 10(a) (and in Figure 11 for the graph  $G'$  in the Appendix). In fact, it is more of a counter-argument, illustrated in Figure 10(b), to the intuition of Figure 1 in [17].

For simplicity, since  $G_{\text{driver}}, G$  are fixed, we shall refer the system Hamiltonian by  $\text{SysH}(J_{\text{xx}})$  for each  $J_{\text{xx}}$ .

Since  $\text{SysH}(0) = \text{SysH}(\mathcal{H}_X)$  is stoquastic, by continuity, there exists a  $J_{\text{xx}}^{\text{single}} > 0$  such that  $\text{SysH}(J_{\text{xx}})$  is eventually stoquastic, for  $J_{\text{xx}} \in (0, J_{\text{xx}}^{\text{single}}]$ . Thus for,  $J_{\text{xx}} \in [-J_{\text{xx}}^{\text{single}}, J_{\text{xx}}^{\text{single}}]$ , the ground state coefficients  $c_i(s) \geq 0$  for all  $i$  and all  $s \in [0, 1]$ .

**Observation 1.** For sufficiently small  $J_{\text{xx}} > 0$ ,  $\text{SysH}(J_{\text{xx}})$  can be seen as a perturbed Hamiltonian from  $\text{SysH}(0)$ , where the perturbation  $V = J_{\text{xx}}(1-s)s \sum_{ij \in G_{\text{driver}}} \sigma_i^x \sigma_j^x$ . The entire evolution of  $\text{SysH}(J_{\text{xx}})$  is a perturbed evolution of  $\text{SysH}(0)$ . In particular, the  $(L, R)$ -ANTI-CROSSING of  $\text{SysH}(0)$  at  $s_x$  also evolves. Observe that

$$\begin{cases} \mathcal{E}_{L_0}(J_{\text{xx}}, s_x^-) = \mathcal{E}_{L_0}(0, s_x^-) + (1 - s_x^-)s_x^- J_{\text{xx}} \sum_{ij \in G_{\text{driver}}} c_i(s)c_j(s) \\ \mathcal{E}_{L_1}(J_{\text{xx}}, s_x^+) = \mathcal{E}_{L_1}(0, s_x^+) + (1 - s_x^+)s_x^+ J_{\text{xx}} \sum_{ij \in G_{\text{driver}}} d_i(s)d_j(s) \end{cases} \quad (8)$$

while  $\mathcal{E}_{R_0}(J_{\text{xx}}, s_x^+) = \mathcal{E}_{R_0}(0, s_x^+), \mathcal{E}_{R_1}(J_{\text{xx}}, s_x^-) = \mathcal{E}_{R_1}(0, s_x^-)$  because there are no **XX**-couplers within  $R$  in  $G_{\text{driver}}$ . For  $J_{\text{xx}} > 0$ ,  $\mathcal{E}_{L_0}(J_{\text{xx}}, s_x^-) > \mathcal{E}_{L_0}(0, s_x^-), \mathcal{E}_{L_1}(J_{\text{xx}}, s_x^+) > \mathcal{E}_{L_1}(0, s_x^+)$  because  $c_i(s) > 0, c_j(s) > 0$  and  $\text{sgn}(c_i(s)c_j(s)) = \text{sgn}(d_i(s)d_j(s))$ . This results in a weaker  $(L', R')$ -ANTI-CROSSING at  $s'_x < s_x$  with a larger  $\delta' > \delta$ , and  $L \subseteq L'$  and  $R \subseteq R'$ . Consequently,  $\text{AC-Gap}(J_{\text{xx}}) = \Theta(\zeta^{\text{dist}_{H'_D}(L', R')}) > \text{AC-Gap}(0)$  because  $\zeta' > \zeta$  and  $\text{dist}_{H'_D}(L', R') \leq \text{dist}_{H_D}(L, R)$ . Conversely,  $-J_{\text{xx}} < 0$ ,  $\mathcal{E}_{L_0}(-J_{\text{xx}}, s_x^-) < \mathcal{E}_{L_0}(0, s_x^-), \mathcal{E}_{L_1}(-J_{\text{xx}}, s_x^+) < \mathcal{E}_{L_1}(0, s_x^+)$ , and it results in a stronger  $(L'', R'')$ -ANTI-CROSSING at  $s''_x > s_x$  with a smaller  $\delta'' < \delta$ , and  $L'' \subseteq L$  and  $R'' \subseteq R$  such that  $\text{AC-Gap}(0) > \text{AC-Gap}(-J_{\text{xx}})$ . That is, we have  $\text{AC-Gap}(-J_{\text{xx}}) < \text{AC-Gap}(0) < \text{AC-Gap}(+J_{\text{xx}})$ . See Figure 8 for an example. By continuity, for  $J_{\text{xx}} \in [-J_{\text{xx}}^{\text{single}}, J_{\text{xx}}^{\text{single}}]$ ,  $\text{AC-Gap}(J_{\text{xx}})$  increases as  $J_{\text{xx}}$  increases. See Figure 10 of a plot of  $\text{AC-Gap}$  vs  $J_{\text{xx}}$  for  $\text{SysH}(J_{\text{xx}}, G_{\text{driver}}, G)$ .

<sup>8</sup>The driver graph actually only needs to be a subgraph of  $G|_L$ , which can be efficiently identified.

**Observation 2.** If there is a  $J_{xx}$  such that  $L$  is an arm of an anti-crossing in **PNStoq**  $\text{SysH}(G, J_{xx}, G_{\text{driver}})$ , then  $L$  will be split into  $L^+$  and  $L^-$ , with the coefficients for states in  $L^+$  ( $L^-$  resp.) being positive (negative resp.).

Notice that

$$\mathcal{E}_{L_0}(J_{xx}, s) = (1-s)sJ_{xx} \sum_{kk' \in G_{\text{driver}}} c_k(s)c_{k'}(s) + \sum_{k \in L^+ \cup L^-} |c_k|^2 E_k \quad (9)$$

Since  $J_{xx} > 0$ ,  $\mathcal{E}_{L_0}(J_{xx}, s)$  is minimized when  $L$  is split into  $L^+$  and  $L^-$  such that  $c_k(s)c_{k'}(s) < 0$  for  $k \in L^+, k' \in L^-$ . See Figure 7 for an illustration.

Furthermore, if we assume that  $t_i \leq 2$ ,  $L$  can be split into  $L^+$  and  $L^-$  such that the only  $XX$ -neighboring is between  $L^+$  and  $L^-$ . That is, there are no  $XX$ -neighboring within  $L^+$  or  $L^-$ . By *XX-neighboring* we mean that there is exactly one  $XX$ -coupler between the two states. Since  $|E_1(s)\rangle \approx |E_R(s)\rangle$  for  $s \in [s_1(J_{xx}), s_2(J_{xx})]$ , there can no be an anti-crossing between the first level and the second level during this interval. However, this does not immediately imply that the second-level gap is large, which is required in order to apply DQA-GS successfully. The second-level gap can still be small if the second-level energy  $E_2(s)$  is close to  $E_1(s) \approx E_R(s)$  for  $s \in [s_1, s_2]$ . However, it is likely that the second level energy  $E_2(s)$  will be different for different  $J_{xx}$  while the first level energy  $E_1(s)$  is independent with  $J_{xx}$ . Therefore, there is a  $J_{xx} \in (J_{xx}^{\text{merge}}, J_{xx}^{\text{double}}]$  such that the second-level gap is large.

**Observation 3.** There exist  $J_{xx}^{\text{split}} > 0$  and  $s_c$  such that  $\text{SysH}(J_{xx}^{\text{split}})$  has two anti-crossings bridged by  $(L^+, L^-)$ , namely,  $(R, L)$ -ANTI-CROSSING at  $s_1 = s_c - \varepsilon$  and  $(L, R)$ -ANTI-CROSSING at  $s_2 = s_c + \varepsilon$  for some  $\varepsilon > 0$ . By the condition that  $\mathcal{E}_{L_0}(J_{xx}^{\text{split}}, s_c) \approx \mathcal{E}_{R_0}(J_{xx}^{\text{split}}, s_c) \approx \mathcal{E}_{R_0}(0, s_x)$ , we obtain  $J_{xx}^{\text{split}} \approx \frac{\overline{E_L} - \overline{E_R}}{(1-s_x) \sum_{ij \in G_{\text{driver}}} c_i(s_c)c_j(s_c)} \geq \overline{E_L} - \overline{E_R}$ , where  $s_c \approx s_x$ . As  $J_{xx}^{\text{split}}$  decreases, there is a sharp exchange between the ground and first excited states and the two anti-crossings are merged, resulting in no AC at  $J_{xx}^{\text{merge}} = J_{xx}^{\text{split}} - \epsilon$ . See Figure 9 for an illustration. As  $J_{xx}$  increases from  $J_{xx}^{\text{split}}$ , the bridge length  $2\varepsilon$  increases, the first AC weakens slightly, while the second AC strengthens slightly. There exists a  $J_{xx}^{\text{double}} > J_{xx}^{\text{split}}$ , such that when  $J_{xx} > J_{xx}^{\text{double}}$ , the first AC is too weak to be qualified as an anti-crossing.

**$L$  and  $R$  share some common vertices.** In our example, for illustrative purpose,  $L$  and  $R$  are not only disjoint subsets of  $2^{[N]}$ , but they are also disjoint in the ground set. However, this is not a required condition, as shown in  $G'$  in Figure 4(b) where the vertex 9 appears both in a local minimum set and the global minimum. This is an important feature for otherwise the problem would be solved efficiently classically by solving  $G \setminus L$ .

**Nested double-ACs or a double multi-level AC.** When there is a  $t_i > 2$ , we take *all* the edges in the independent-cliques as the driver graph. However, in this case, there may be an AC between the first excited state and higher and we no longer can guarantee the large second-level gap. Instead, it may have a sequence of nested double-ACs (as shown in Figure 5(f)) or a double multi-level anti-crossing where the lowest excited states form a narrow band, as shown in Figure 13(a) in the Appendix for the 15-qubit instance in [10]. In this case, the system would undergo diabatic transitions to the higher excited states through a sequence of the first ACs of the nested double-ACs (or through the first AC of a double multi-level AC), and then returns to the ground state through the sequence of second ACs of the nested double-ACs (or through the second AC of a double multi-level AC). More details of the relationship between the driver graph structure and the nested double-ACs (or double multi-level ACs) will be reported in our subsequent work.

**Rules for constructing the driver graph.** In our above Claim, the driver graph  $G_{\text{driver}}$  is taken to be  $G|_L$ . Our arguments for the Observations actually reveal the intuition for constructing the driver graph. Namely, the idea is to include the XX-couplers between local minima in  $L$  (so to cause the split) and avoid including XX-couplers that are coupling states in  $R$  and its neighbors (so as not to weaken  $\mathcal{E}_{R_0}$ ). We impose the independent-cliques structure in the local minima for the reason of justification, and also for the efficacy of identifying  $G|_L$  with partial information of  $L$ , to be elaborated in the next section. We note that it is possible to relax the independent-cliques condition to *almost-independent-cliques* by allowing some edges between these cliques.

### 2.2.3 A General Procedure without Prior Knowledge of the Problem Structure

A natural question is: without knowing the problem structure, can one design an appropriate driver graph efficiently? As we note above, for the instances that we are considering, knowing the set  $L$  (without any knowledge of  $R$ ) will be sufficient to construct the appropriate driver graph. The idea follows that if we can identify some elements in  $L$  (which is possible because these are the “wrong answers” from QA), with the special independent-cliques structure, it is possible to recover  $G|_L$  explicitly and  $L$  implicitly (as  $L$  may consist of exponentially many maximal independent sets) by exploring the graph locally with a classical procedure. More specifically, since we assume that the instance has an  $(L, R)$ -ANTI-CROSSING when running with the stoquastic QA algorithm, and if we further assume that the  $(L, R)$ -ANTI-CROSSING is the only super-polynomially small-gap in the system Hamiltonian, then with polynomial time, either by a stoquastic quantum annealer, or the simulated quantum annealing (SQA) [27, 28], one can identify at least one local minimum  $l_0$  in  $L$ . We then identify  $G|_L$  through  $l_0$  as follows. First, for each vertex  $v$  in  $l_0$ , we find the maximum clique that contains  $v$  (that is, all the high-weight vertices that are adjacent to  $v$  and each other), and is independent of other elements in  $l_0$ . Then we eliminate the vertices in the cliques found that are adjacent to some vertices in another clique. This can be done according to the descending order of the clique-degree (i.e. number of cliques the vertex is adjacent to) of the vertices, breaking ties according to the vertex-weight. This way we obtain a set of independent cliques  $G_{IC}$  that contains  $l_0$ . For example, the  $G_{IC}$  so discovered through a seed  $l_0 = \{1, 3, 6\}$  in Figure 4(b) will be the same as  $G|_L$ . Intuitively, if  $G|_L$  has a “clear cut boundary” (i.e. no ambiguous vertex which connects two cliques), we have  $G_{IC} = G|_L$ . It remains to be shown that under what conditions,  $G_{IC}$  (which can be improved by providing more local minima in  $L$ , and/or when we relax to allow almost-independent cliques) is the same as  $G|_L$ .

In order to find an appropriate  $J_{xx}$ , we obtain an upper bound for the MWIS (corresponds to  $-\overline{E^R}$ ). Such a good upper bound can be obtained through a weighted clique cover as used in the branch-and-bound algorithm for MWIS [24, 25, 26]. Together with the estimate bound for  $\overline{E_L}$ , we obtain a possible range  $(0, U]$  for  $J_{xx}$ . We then try  $p$  polynomial number of different  $J_{xx}$  within the range  $(0, U]$ , by running  $\text{SysH}(G, J_{xx}, G_{\text{driver}})$  diabatically in polynomial time and record the best answer.

The algorithm, which we name DIC-DAC-DOA, is summarized in the following:

1. Find an  $l_0 \in L$  in polynomial time using either a stoquastic quantum annealer, or a simulated quantum annealing (SQA) algorithm;
2. Find an independent-cliques structure around  $l_0$  in  $G$ ,  $G_{IC}$ , and obtain an estimate of  $-\overline{E_L}, U_L$ ;
3. Obtain an upper bound for  $-\overline{E_R}, U_R$ , e.g. using a weighted clique cover.
4. Let  $G_{\text{driver}} = G_{IC}$ ;  $U = u(U_R - U_L)$  for some constant  $u \geq 1$ .
5. Let  $p$  be a pre-determined polynomial number. For  $i = 1$  to  $p$ , let  $J_{xx} = i/pU$ , run  $\text{SysH}(G, J_{xx}, G_{\text{driver}})$  diabatically in polynomial time and record each returned answer;

6. Return the best answer.

(In practice, we may need to try many different ranges of values with different  $p$  in a manner similar to the binary search, until the returned answers converge.)

**Quantum Speedup.** If the instance has the independent-cliques structure such that  $G_{IC} = G|_L$ , and there is a  $J_{xx} \in (0, U]$  such that there is a double-AC in  $\text{SysH}(J_{xx}, G_{\text{driver}}, G)$  as described in Claim (II), the above algorithm DIC-DAC-DOA will successfully find the ground state through DQA in polynomial time, with an  $O(c^\alpha)$  speedup over the  $(L, R)$ -ANTI-CROSSING plagued stoquastic algorithm where  $\alpha = \text{dist}_{H_D}(L, R)$ . It may have similar speedup for some other classical heuristics that developed in comparison with QA algorithms (see e.g. [28]). While Claim (II) remains to be more rigorously proved, it is worthwhile to point out that the mechanism of achieving speedup here is through a bridged double-AC which requires the necessity of +XX-interactions, so as to overcome the single-AC in the stoquastic case. At the same time, this is achieved through a “cancellation” effect, and not by removing the local minima from the graph as in the classical algorithm. This point perhaps would gain much appreciation when comparing with the classical branch-and-bound solver for the MWIS where a clique cover is pruned. From our perspective, this mechanism of achieving the speedup (by overcoming the local minima) does not seem to have a similar classical counterpart, c.f. [8].

**Remark.** As with successfully resolving our 15-qubit graph from [10] (see an example in Figure 13), we can similarly try to resolve the random instances of the EXACT COVRE 3 (EC3) problem that plagued the stoquastic QA because of the small AC-gap as described in [11]. More specifically, we first convert a random EC3 instance to an MWIS instance according to the reduction described in [29, 12], and then apply the above algorithm DIC-DAC-DOA to the instance. If there is more than one AC in the stoquastic QA (of the MWIS instance), one may be able to solve the problem progressively by resolving one AC at a time.

### 3 Discussion

In this paper, we point out the essential distinction of **EStoq** and **PNStoq** for the non-stoquastic Hamiltonians from the algorithmic perspective. The quantum evolutions of the **EStoq** and **PNStoq** algorithms can be very different, especially when comparing their spectral gaps with their de-signed counterparts. Furthermore, we demonstrate the essentiality of the design of the XX-driver graph (which specifies which XX-couplers to be included) that has not been considered by other previous work.

In particular, we describe a proper-non-stoquastic QA algorithm that can overcome the anti-crossing plagued stoquastic QA algorithm and achieve a quantum speedup for quantum optimization through DQA-GS, with the two essential ingredients: non-stoquastic +XX-couplers and the structure of the XX-driver graph. This is in contrast to the recent comments made in [5] that the non-stoquastic is not essential for quantum enhancement, where neither the distinction of non-stoquasticity nor the structure of driver graph is taken into consideration. The essentiality of the **PNStoq** +XX-couplers comes from the ability to overcome the inevitable single-AC small gap in the stoquastic QA by “splitting” the AC into two bridged ACs (a double-AC) that would then enable DQA-GS to solve the problem efficiently, c.f. [30]. The possibility of constructing the desired driver graph efficiently is because one can make use of the “wrong answers” from the anti-crossing plagued stoquastic QA, together with the imposed special independent-cliques condition. The quantum speedup through the idea of double-AC-enabled-DQA was first proposed in [6], where an *oracular* stoquastic QA algorithm for solving the glued-tree problem in polynomial time is presented. There the double-AC is formed by two identical anti-crossings (due

to the symmetric evolution at the middle). In contrast, our double-AC is formed by two anti-symmetric anti-crossings that share a common arm of the opposite sign as the bridge. As we argue above, the proper-non-stoquastic interactions (which cause the negative amplitudes in the ground state) are essential in our argument to form the bridge. Admittedly, our algorithmic procedure still requires a more rigorous proof, nevertheless, we believe that we have provided enough arguments and evidence that are confirmed by (scalable) numerical examples. In particular, when the hard instances whose local minima subgraph is indeed the same as the graph  $G_{IC}$  discovered by our algorithm DIC-DAC-DOA, then there would be a double-AC or a sequenced of nested double-ACs or a narrow band that enable DQA to solve the problem successfully in polynomial time. This would achieve an exponential speedup over the stoquastic algorithm, and possible exponential speedup over the state-of-the-art classical algorithms for such instances.

Furhtermore, there are some reasons to further support our arguments: (1) We make use of the exclusive quantum feature in our algorithm; (2) The special structure of the instances are believed to one of the obstacles for the efficient classical algorithms (heuristics or exact solvers). (3) Proper-non-stoquastic (with XX-driver) may not be VGP[15], and thus not QMC-simulable.

We have successfully resolved the small-gap instance constructed in [10] (see Figure 13), and it remains to be further investigated that our proposed algorithm DIC-DAC-DOA would also resolve the random EC3 instances described by Altshuler et al in [11].

The insights of this work are obtained based on the novel characterizations of a modified and generalized parametrization definition of an anti-crossing in the context of QOA. We demonstrate how the parametrized AC can be used as a tool to open up the ‘black-box’ of the QOA algorithm, and thus facilitate the analysis and design of adiabatic or diabatic QA algorithms. Furthermore, one can discover some interesting quantum evolution, such as the two anti-crossings merged at  $J_{xx}^{\text{merge}}$ , where a ‘‘sharp exchange’’ occurs not because of an anti-crossing, but due to the merging of two anti-crossings.

There are several future works to be followed: (1) There are several different ways to improve the design of the driver graph, including obtaining more local minima that are part of  $L$ ; and relaxing the independent-cliques condition to the almost-independent-cliques such that some edges between cliques are allowed (these edges are not necessarily needed to be included in the driver graph). (2) We can consider the possible generalization of the AC definition to include a multi-level anti-crossing such that the anti-crossing is between one energy level and a band of of closely tie together energy levels (a pseudo degenerate state) which can make the analysis of the algorithm more robust. (3) There is an **ESToq**  $J_{xx}$  such that the min-gap is a weak non-AC gap that is larger than the original AC-gap. Before proper-non-stoquastic XX-couplers to be built, if **ESToq** is VGP, then we have a quantum-inspired algorithm that is faster than the stoquastic quantum algorithm, once a QMC-simulation algorithm for VGP is developed. Finally, the problem of the *intertwined sparse* universal hardware graph and the minor-embedding problem [31, 32], including both problem graph and driver graph, will be addressed next.

## 4 Methods

### 4.1 Proof of Proposition 2.2

*Proof.* (of Proposition 2.2) The derivation is based on the assumption of the linear interpolation between  $H_D$  (driver Hamiltonian) and  $H_P$  (problem Hamiltonian). That is,  $H(s) = (1 - s)H_D + sH_P$ . (The catalyst version will be approximated.) Note that we can write  $H(s) = H(s_x) + (s - s_x)(H_P - H_D)$ . The idea is based on the non-degenerate perturbation theory where the unperturbed Hamiltonian  $H^{(0)} = H(s_x)$ , and the perturbation  $\delta H(= \frac{\delta H}{\delta s}) = H_P - H_D$ . We apply the perturbation to  $H(s_x + \lambda) = H(s_x) + \lambda\delta H$ , where  $|\lambda|$  is sufficiently small. (The standard non-degenerate perturbation theory usually apply to the positive small  $\lambda$ . See e.g. [22].

Here we apply to both positive and negative  $\lambda$ . For the small negative  $\lambda$ , one can think of it as it equivalently applies the negative sign to  $\delta H$ .) From the perturbation theory (see, e.g. [22] Chapter 1 page 8), we have the states and energies for  $H(\lambda) = H(s_x) + \lambda\delta H$ :

$$\begin{cases} |E_n(s_x + \lambda)\rangle = |E_n(s_x)\rangle - \lambda \sum_{k \neq n} \frac{\delta H_{kn}(s_x)}{E_k(s_x) - E_n(s_x)} |E_k(s_x)\rangle + O(\lambda^2) \\ E_n(s_x + \lambda) = E_n(s_x) + \lambda \delta H_{nn}(s_x) - \lambda^2 \sum_{k \neq n} \frac{|\delta H_{kn}(s_x)|^2}{E_k(s_x) - E_n(s_x)} + O(\lambda^3) \end{cases} \quad (10)$$

where  $\delta H_{mn}(s_x) \equiv \langle E_m(s_x) | \delta H | E_n(s_x) \rangle$ . By definition (condition (a)),  $\Delta_{10}(s_x) = E_1(s_x) - E_0(s_x) \ll E_2(s_x) - E_0(s_x) = \Delta_{20}(s_x)$ , and  $|\lambda|$  is sufficiently small, we apply the above formulae to  $n = 0, 1$  and obtain:

$$\begin{cases} |E_0(s_x + \lambda)\rangle \simeq |E_0(s_x)\rangle - \lambda \frac{\delta H_{10}(s_x)}{\Delta_{10}(s_x)} |E_1(s_x)\rangle \\ |E_1(s_x + \lambda)\rangle \simeq |E_1(s_x)\rangle + \lambda \frac{\delta H_{10}(s_x)}{\Delta_{10}(s_x)} |E_0(s_x)\rangle \end{cases} \quad (11)$$

and

$$\begin{cases} E_0(s_x + \lambda) \doteq E_0(s_x) + \lambda \delta H_{00}(s_x) - \lambda^2 \frac{|\delta H_{10}(s_x)|^2}{\Delta_{10}(s_x)} \\ E_1(s_x + \lambda) \doteq E_1(s_x) + \lambda \delta H_{11}(s_x) + \lambda^2 \frac{|\delta H_{10}(s_x)|^2}{\Delta_{10}(s_x)} \end{cases} \quad (12)$$

[where the error tolerance in  $\doteq$  due to perturbation is  $\epsilon_p \ll \Delta_{10}(s_x)/\Delta_{20}(s_x)$ .] Eq.(12) thus gives rise to the two parabolas with  $B_0 = \delta H_{00}(s_x)$  and  $B_1 = \delta H_{11}(s_x)$  and  $A = \frac{|\delta H_{kn}(s_x)|^2}{\Delta_{10}(s_x)} > 0$ . This proves Property (C1).

From Eq. (11), for all  $k \in \tilde{L} \cup \tilde{R}$ , we have

$$\begin{cases} c_k(s_x + \lambda) \doteq c_k(s_x) - \lambda \frac{\delta H_{10}(s_x)}{\Delta_{10}(s_x)} d_k(s_x) \\ d_k(s_x + \lambda) \doteq d_k(s_x) + \lambda \frac{\delta H_{10}(s_x)}{\Delta_{10}(s_x)} c_k(s_x) \end{cases} \quad (13)$$

for  $\lambda \in [-\delta, \delta]$  (the error tolerance in  $\doteq$  is  $\epsilon_p$ ).

From condition (iv), we have  $|L_0(s - \delta)| \approx 1 - \gamma$  while  $|L_0(s + \delta)| \approx 0$ , we have  $|c_l(s)| \downarrow$ ; and  $|L_1(s + \delta)| \approx 1 - \gamma$  while  $|L_1(s - \delta)| \approx 0$ , we have  $|d_l(s)| \uparrow$ , for all  $l \in L$ . Similarly, we have  $|c_r(s)| \uparrow$ ,  $|d_r(s)| \downarrow$ , for all  $r \in R$ . This proves Property (C2).

To show Property (C3), we distinct two possible cases: (1)  $\delta H_{10}(s_x) > 0$  and (2)  $\delta H_{10}(s_x) < 0$ . Assume case (1), i.e.  $\delta H_{10}(s_x) > 0$ . For  $l \in L$ , from the above arguments for Property (C2), we  $|c_l(s)| \downarrow$ ,  $|d_r(s)| \uparrow$ , i.e.  $|c_l(s)|$  is decreasing while  $|d_r(s)|$  is increasing. By Eq. (13),  $c_l(s)$  must be in the same sign of  $d_l(s)$  (i.e.  $c_l(s)d_l(s) > 0$ ) (otherwise both would be increasing, a contradiction.) Similarly, we can deduce that  $c_r(s)d_r(s) < 0$  for  $r \in R$ . That is, we have

$$\begin{cases} L_0 \text{ and } L_1 \text{ in the same sign: } \text{sgn}(c_l(s))\text{sgn}(d_l(s)) = +1 \text{ for all } l \in L \\ R_0 \text{ and } R_1 \text{ in the opposite sign: } \text{sgn}(c_r(s))\text{sgn}(d_r(s)) = -1 \text{ for all } r \in R \end{cases}$$

where  $s : s_x - \delta \rightsquigarrow s_x + \delta$ .

Similarly, we can show that for case (2):

$$\begin{cases} L_0 \text{ and } L_1 \text{ in the opposite sign: } \text{sgn}(c_l(s))\text{sgn}(d_l(s)) = -1 \text{ for all } l \in L \\ R_0 \text{ and } R_1 \text{ in the same sign: } \text{sgn}(c_r(s))\text{sgn}(d_r(s)) = +1 \text{ for all } r \in R \end{cases}$$

where  $s : s_x - \delta \rightsquigarrow s_x + \delta$ . This proves Property (C3).



To prove Property (C4), substitute  $\lambda = -\delta, +\delta$  to Eq. (13), we get

$$\begin{cases} c_k(s_x - \delta) \doteq c_k(s_x) + \delta \frac{\delta H_{10}(s_x)}{\Delta_{10}(s_x)} d_k(s_x) \\ c_k(s_x + \delta) \doteq c_k(s_x) - \delta \frac{\delta H_{10}(s_x)}{\Delta_{10}(s_x)} d_k(s_x) \end{cases}$$

Summing up the above two equations, we get  $2c_k(s_x) \doteq c_k(s_x - \delta) + c_k(s_x + \delta)$ . Similarly,  $2d_k(s_x) \doteq d_k(s_x - \delta) + d_k(s_x + \delta)$ . By the full-exchange condition in Eq.(3), we have  $|c_k(s_x - \delta)| \doteq |d_k(s_x + \delta)|$  and  $|c_k(s_x + \delta)| \doteq |d_k(s_x - \delta)|$ , consequently we have  $|c_k(s_x)| \doteq |d_k(s_x)|$ . This proves Property (C4).  $\square$

**Remark on the proof.** This derivation is based on the linear interpolation path. However, for the catalyst, we can similarly apply the arguments to the linear approximation near the anti-crossing point, with  $\delta H = H_P - s_x H_D$ .

### Proofs of AC-gap Bound

*Proof.* (of Lemma 2.3) By definition,  $E_i(s_x) = \langle E_i(s_x) | H(s_x) | E_i(s_x) \rangle$  for  $i = 0, 1$ . Thus, we have

$$\Delta_{10}(s_x) = \langle E_1(s_x) | H(s_x) | E_1(s_x) \rangle - \langle E_0(s_x) | H(s_x) | E_0(s_x) \rangle \quad (14)$$

We assume that the anti-crossing is  $(1 - \epsilon_v)$ -full-exchange and it satisfies the approximate SAS property in (C4).

First, we show that if the SAS is exact, i.e.,

$$(*) \begin{cases} |E_0(s_x)\rangle = |\tilde{L}(s_x)\rangle + |\tilde{R}(s_x)\rangle \\ |E_1(s_x)\rangle = |\tilde{L}(s_x)\rangle - |\tilde{R}(s_x)\rangle \end{cases}$$

the AC-Gap is contributed from the coefficients of negligible states. Substitute (\*) into Eq. (14), because of the cancellation of the opposite terms, we have  $|E_0(s_x)\rangle = -4\langle \tilde{L}(s_x) | H(s_x) | \tilde{R}(s_x) \rangle$ . By assumption that  $\tilde{L} \cap \tilde{R} = \emptyset$ , we have  $\langle \tilde{L}(s_x) | H_P | \tilde{R}(s_x) \rangle = 0$ . Thus,  $\Delta_{10}(s_x) \doteq -4(1-s)\langle \tilde{L}(s_x) | H_D | \tilde{R}(s_x) \rangle$ . If  $\text{dist}_{H_D}(L, R) > 3$ , it implies  $\langle L | H_D | R \rangle = 0$ , and thus we have  $\Delta_{10}(s_x) \doteq -4(1-s)\langle n(L)(s_x) | H_D | n(R)(s_x) \rangle$ .

Let  $g(L) = \{i \in n(L) : \exists j \in n(R) \text{ s.t. } \langle i | H_D | j \rangle \neq 0\}$ ,  $g(R) = \{j \in n(R) : \exists i \in n(L) \text{ s.t. } \langle i | H_D | j \rangle \neq 0\}$  be the set of states that contribute non-zero values to the gap.

That is,

$$\begin{aligned} \Delta_{10}(s_x) &= \kappa \langle g(L)(s_x) | H_D | g(R)(s_x) \rangle \\ &= \kappa \sum_{i \in g(L), j \in g(R), \langle i | H_D | j \rangle \neq 0} c_i(s_x) c_j(s_x) \langle i | H_D | j \rangle \\ &= \kappa \sum_{i \in g(L), j \in g(R), \langle i | H_D | j \rangle \neq 0} d_i(s_x) d_j(s_x) \langle i | H_D | j \rangle \end{aligned}$$

where  $\kappa = -4(1-s)$ . When the AC is  $(1 - \epsilon_v)$ -full-exchange, the small error due to the differences in  $c, d$  of the non-negligible states is absorbed by the above term.  $\square$

- Remark: As the AC becomes weaker, the error term due to the difference in  $c, d$  of the non-negligible states can be large enough to dominate the gap size, in this case the min-gap will be  $\omega(\zeta^\alpha)$  (strictly greater than the order of  $\zeta^\alpha$ ).

*Proof.* (of Theorem 2.4) First, assume the anti-crossing is near the end of annealing (i.e.  $s_x \approx 1$ ) (with  $R$  as the ground state, and  $L$  as the first excited state) as in the perturbative crossing case.

Observe that: For  $k \in n(R)$ :  $c_k(s_x - \delta) \neq 0 \rightarrow c_k(s_x + \delta) = 0$ , we have  $c_k(s_x) \doteq 1/2c_k(s_x - \delta)$ .

For  $k \in n(L)$ : we have  $d_k(s_x - \delta) \neq 0 \rightarrow d_k(s_x + \delta) = 0$ , thus  $c_k(s_x) \doteq d_k(s_x) \doteq 1/2d_k(s_x - \delta)$ .

Both  $c_k(s_x - \delta)$  and  $d_k(s_x - \delta)$  can be computed from the high-order corrections using Brillouin-Wigner perturbation theory [23]. Let  $H(\lambda) = H_P + \lambda H_D$ , where the unperturbed problem Hamiltonian  $H_P$ , while the perturbation Hamiltonian is  $H_D$ . The high order corrections of the perturbed state is given by

$$\begin{aligned} |E_n(\lambda)\rangle = & |n\rangle + \lambda \sum_{m_1 \neq n} |m_1\rangle \frac{\langle m_1 | H_D | n \rangle}{E_n(\lambda) - E_{m_1}} + \lambda^2 \sum_{m_1 \neq n} \sum_{m_2 \neq n} |m_1\rangle \frac{\langle m_1 | H_D | m_2 \rangle \langle m_2 | H_D | n \rangle}{(E_n(\lambda) - E_{m_1})(E_n(\lambda) - E_{m_2})} + \dots \\ & + \lambda^k \sum_{m_1 \neq n} \sum_{m_2 \neq n} \dots \sum_{m_k \neq n} |m_1\rangle \frac{\langle m_1 | H_D | m_2 \rangle \langle m_2 | H_D | m_3 \rangle \dots \langle m_k | H_D | n \rangle}{(E_n(\lambda) - E_{m_1})(E_n(\lambda) - E_{m_2}) \dots (E_n(\lambda) - E_{m_k})} + \dots \end{aligned}$$

where  $E_n(\lambda)$  in the denominator is the (unknown) energy of the  $|E_n(\lambda)\rangle$ .

We apply the above perturbation formula to the ground state ( $R$ ) to compute  $c_k(s_x)$  for  $k \in n(R)$ , and to the first excited state ( $L$ ) to compute  $c_k(s_x)$  for  $k \in n(L)$ . [Using  $\mathcal{E}_{R_0}(s_x^+)$  or  $\mathcal{E}_{L_0}(s_x^-)$  for  $E_n(\lambda)$ .]

The coefficients decrease in an almost geometric order, that is,  $c_k \approx a^k$  with  $0 < a < 1$ ,  $d_k \approx b^k$  with  $0 < b < 1$ . The larger  $k$  ( $H_D$ -driver distance) the smaller the coefficients. Therefore it is the pairs with smallest distance  $t$  (corresponding to the  $t!$  shortest paths) between  $L, R$  that dominate the gap size in Eq. (7) of Lemma, where  $t = \text{dist}_{H_D}(L, R)$ .

For the case that  $s_x \ll 1$ , we can however shift the anti-crossing to near the end, using the scaling theorem in [4].

The above argument can be generalized (by re-deriving Brillouin-Wigner perturbation theory) to include when  $L$  consists of the almost degenerate first excited states, and/or  $R$  consists of GS and its LENS, when the property that coefficients decrease in geometric order of its distance still holds.  $\square$

## References

- [1] T. Albash and D.A. Lidar. Adiabatic Quantum Computation. *Rev. Mod. Phys.* 90, 015002, 2018.
- [2] Sergey Bravyi, David P. Divincenzo, Roberto Oliveira, and Barbara M. Terhal. The complexity of stoquastic local hamiltonian problems, *Quantum Info. Comput.* 8, 361–385, 2008.
- [3] T. Albash. Role of Non-stoquastic Catalysts in Quantum Adiabatic Optimization. *Phys. Rev. A.*, 99, 042334, 2019.
- [4] V. Choi. The Effects of the Problem Hamiltonian Parameters on the Minimum Spectral Gap in Adiabatic Quantum Optimization. *Quantum Inf. Processing.*, 19:90, 2020. *arXiv:quant-ph/1910.02985*.
- [5] E.J. Crosson and D.A. Lidar. Prospects for Quantum Enhancement with Diabatic Quantum Annealing. *arXiv:2008.09913v1*, 2020.
- [6] R.D. Somma, D. Nagaj and M. Kieferova. Quantum Speedup by Quantum Annealing, *Phys. Rev. Lett.* 109, 050501, 2012.
- [7] Siddharth Muthukrishnan, Tameem Albash, Daniel A. Lidar. Sensitivity of quantum speedup by quantum annealing to a noisy oracle, *Phys. Rev. A* 99, 032324, 2019.

- [8] S. Muthukrishnan, T. Albash, and D.A. Lidar. Tunneling and speedup in quantum optimization for permutation-symmetric problems. *Phys. Rev. X*, 6, 031010, 2016.
- [9] S. Jansen, M.-B. Ruskai, and R. Seiler, Bounds for the adiabatic approximation with applications to quantum computation. *J. Math. Phys.* 48, 102111 (2007).
- [10] M.H.S. Amin, V. Choi. First order phase transition in adiabatic quantum computation. *arXiv:quant-ph/0904.1387*. *Phys. Rev. A.*, 80 (6), 2009.
- [11] B. Altshuler, H Krovi, J Roland. Anderson localization makes adiabatic quantum optimization fail. *Proc Natl Acad Sci USA*, 107:12446–12450, 2010.
- [12] V. Choi. Different Adiabatic Quantum Algorithms for the NP-Complete Exact Cover Problem. *Proc Natl Acad Sci USA*, 108(7): E19-E20, 2011.
- [13] M. Wilkinson, Statistics of multiple avoided crossings. *J. Phys. A: Math. Gen.*, 22, 2795-2805, 1989.
- [14] M. A. Qureshi, J. Zhong, P. Mason, J. J. Betouras, and A. M. Zagoskin. Pechukas-Yukawa formalism for Landau-Zener transitions in the presence of external noise. *arXiv:1803.05034v2*, 2018.
- [15] Itay Hen. Determining QMC simulability with geometric phases. <https://arxiv.org/abs/2012.02022>.
- [16] Milad Marvian, Daniel A. Lidar, and Itay Hen, On the computational complexity of curing non-stoquastic hamiltonians, *Nature Communications* 10, 1571, 2019.
- [17] Elizabeth Crosson, Tameem Albash, Itay Hen, A. P. Young. De-Signing Hamiltonians for Quantum Adiabatic Optimization. *Quantum* 4, 334 (2020).
- [18] Michael Jarret, Stephen P. Jordan. Adiabatic optimization without local minima *Quantum Information and Computation*, Vol. 15 No. 3/4 pg. 181-199 (2015).
- [19] Michael Jarret. Hamiltonian surgery: Cheeger-type gap inequalities for nonpositive (stoquastic), real, and Hermitian matrices. <https://arxiv.org/abs/1804.06857>.
- [20] Dimitrios Noutsos, On Perron-Frobenius property of matrices having some negative entries, *Linear Algebra and its Applications*, 412, 132–153, 2006.
- [21] A. Elhashash and D.B. Szyld. On general matrices having the Perron-Frobenius Property, *Electronic Journal of Linear Algebra*, Volume 17, 2008.
- [22] Barton Zwiebach. 8.06 Quantum Physics III. Spring 2018. Massachusetts Institute of Technology: MIT OpenCourseWare, <https://ocw.mit.edu>. License: Creative Commons BY-NC-SA.
- [23] Robert Littlejohn. Bound-State Perturbation Theory, Physics 221A, Fall 2019, Notes 22., <http://bohr.physics.berkeley.edu/classes/221/1112/notes/perth.pdf>
- [24] S. Held, W. Cook, & E.C. Sewell. Maximum-weight stable sets and safe lower bounds for graph coloring, *Math. Prog. Comp.* 4, 363–381 (2012).
- [25] J. Warren, I. Hicks. Combinatorial branch-and-bound for the maximum weight independent set problem. Technical report, Texas A&M University (2006). Available at <http://www.caam.rice.edu/~ivhicks/jeff.rev.pdf>

- [26] E. Balas, J. Xue. Weighted and unweighted maximum clique algorithms with upper bounds from fractional coloring. *Algorithmica* 15, 397–412 (1996).
- [27] G. E.Santoro, R. Martonak, E. Tosatti, and R. Car, Theory of quantum annealing of an Ising spin glass, *Science* 295, 2427–2430 (2002).
- [28] I. Hen, J. Job, T. Albash, T. F. Rønnow, M. Troyer, and D. Lidar. Probing for quantum speedup in spin glass problems with planted solutions, *Phys. Rev. A* 92, 042325 (2015).
- [29] V. Choi. Different Adiabatic Quantum Algorithms for the NP-Complete Exact Cover and 3SAT Problem. *Quantum Information and Computation*, Vol. 11, 0638–0648, 2011.
- [30] E. Crosson and J. Bowen, Quantum ground state isoperimetric inequalities for the energy spectrum of local Hamiltonians. *arXiv:1703.10133* (2017).
- [31] V. Choi. Minor-embedding in adiabatic quantum computation: I. The parameter setting problem. *Quantum Inf. Processing.*, 7, 193–209, 2008.
- [32] V. Choi. Minor-embedding in adiabatic quantum computation: II. Minor-universal graph design. *Quantum Inf. Processing.*, 10, 343–353, 2011.
- [33] Huo Chen, Daniel A. Lidar. HOQST: Hamiltonian Open Quantum System Toolkit <https://arxiv.org/abs/2011.14046>, 2020.

## Appendix

### A Maximum-Weight Independent Set (MWIS) Problem

The Maximum-Weight Independent Set (MWIS) problem (optimization version) is defined as:

**Input:** An undirected graph  $G(= (V(G), E(G)))$ , where each vertex  $i \in V(G) = \{1, \dots, n\}$  is weighted by a positive rational number  $w_i$

**Output:** A subset  $S \subseteq V(G)$  such that  $S$  is independent (i.e., for each  $i, j \in S, i \neq j, ij \notin E(G)$ ) and the total *weight* of  $S$  ( $= \sum_{i \in S} w_i$ ) is maximized. Denote the optimal set by  $\text{mis}(G)$ .

We recall a quadratic binary optimization formulation (QUBO) of the problem. More details can be found in [31].

**Theorem A.1** (Theorem 5.1 in [31]). *If  $\lambda_{ij} \geq \min\{w_i, w_j\}$  for all  $ij \in E(G)$ , then the maximum value of*

$$\mathcal{Y}(x_1, \dots, x_n) = \sum_{i \in V(G)} w_i x_i - \sum_{ij \in E(G)} \lambda_{ij} x_i x_j \quad (15)$$

*is the total weight of the MIS. In particular if  $\lambda_{ij} > \min\{w_i, w_j\}$  for all  $ij \in E(G)$ , then  $\text{mis}(G) = \{i \in V(G) : x_i^* = 1\}$ , where  $(x_1^*, \dots, x_n^*) = \arg \max_{(x_1, \dots, x_n) \in \{0,1\}^n} \mathcal{Y}(x_1, \dots, x_n)$ .*

Here the function  $\mathcal{Y}$  is called the pseudo-boolean function for MIS, where the boolean variable  $x_i \in \{0, 1\}$ , for  $i = 1, \dots, n$ . The proof is quite intuitive in the way that one can think of  $\lambda_{ij}$  as the *energy penalty* when there is an edge  $ij \in E(G)$ . In this formulation, we only require  $\lambda_{ij} > \min\{w_i, w_j\}$ , and thus there is freedom in choosing this parameter.

## MIS-Ising Hamiltonian

By changing the variables ( $x_i = \frac{1+s_i}{2}$  where  $x_i \in \{0, 1\}$ ,  $s_i \in \{-1, 1\}$ ), it is easy to show that MIS is equivalent to minimizing the following function, known as the *Ising energy function*:

$$\mathcal{E}(s_1, \dots, s_n) = \sum_{i \in \mathcal{V}(G)} h_i s_i + \sum_{ij \in \mathcal{E}(G)} J_{ij} s_i s_j, \quad (16)$$

which is the eigenfunction of the following *Ising Hamiltonian*:

$$\mathcal{H}_{\text{Ising}} = \sum_{i \in \mathcal{V}(G)} h_i \sigma_i^z + \sum_{ij \in \mathcal{E}(G)} J_{ij} \sigma_i^z \sigma_j^z \quad (17)$$

where  $h_i = \sum_{j \in \text{nbr}(i)} \lambda_{ij} - 2w_i$ , (conversely  $w_i = 1/2(\sum_{j \in \text{nbr}(i)} J_{ij} - h_i)$ ),  $J_{ij} = \lambda_{ij}$ ,  $\text{nbr}(i) = \{j : ij \in \mathcal{E}(G)\}$ , for  $i \in \mathcal{V}(G)$ .

For convenience, we will refer to a Hamiltonian in such a form as an *MIS-Ising* Hamiltonian.

## B Resolving the 15-qubit graph $G_{rm}$ in [10]

The example graph from [10] is shown in Figure 12 (a). The stoquastic QA  $\text{SysH}(\mathcal{H}_X, G_{rm})$  has an anti-crossing with a small gap ( $8e - 3$ ), as shown in Figure 12 (b). Taking the three triangles (three independent cliques) as the driver graph  $G_{\text{driver}}$   $\text{SysH}(J_{xx}, G_{\text{driver}}, G_{rm})$  has no anti-crossing for  $J_{xx} \in [0.5, 2.2]$ . In particular, for  $J_{xx} = 2.0$ , min-gap is greater than 0.24 at 0.523, as shown in Figure 13(b). For  $J_{xx} = 2.5$   $\text{SysH}(J_{xx}, G_{\text{driver}}, G_{rm})$  has a double multi-level anti-crossing, as shown in Figure 13(a). DQA-GS can be applied to this example by a diabatic cascade at the first AC and then return to ground state through another diabatic cascade at the second AC. This example also illustrates the difference from DQA in [5] where the system remains in the subspace and does not necessarily return to the ground state.

## Acknowledgments

I would like to thank Jamie Kerman for introducing to me the XX-driver graph problem which directly rekindle this research. Special thanks to Itay Hen for the very helpful discussion and comments and his help. I would like to thank Daniel Lidar for his comments, especially about diabatic cascades, and for the opportunity to participate in DARPA-QEO and DARPA-QAFS programs. Seeking funding and computer resource support to continue this work.

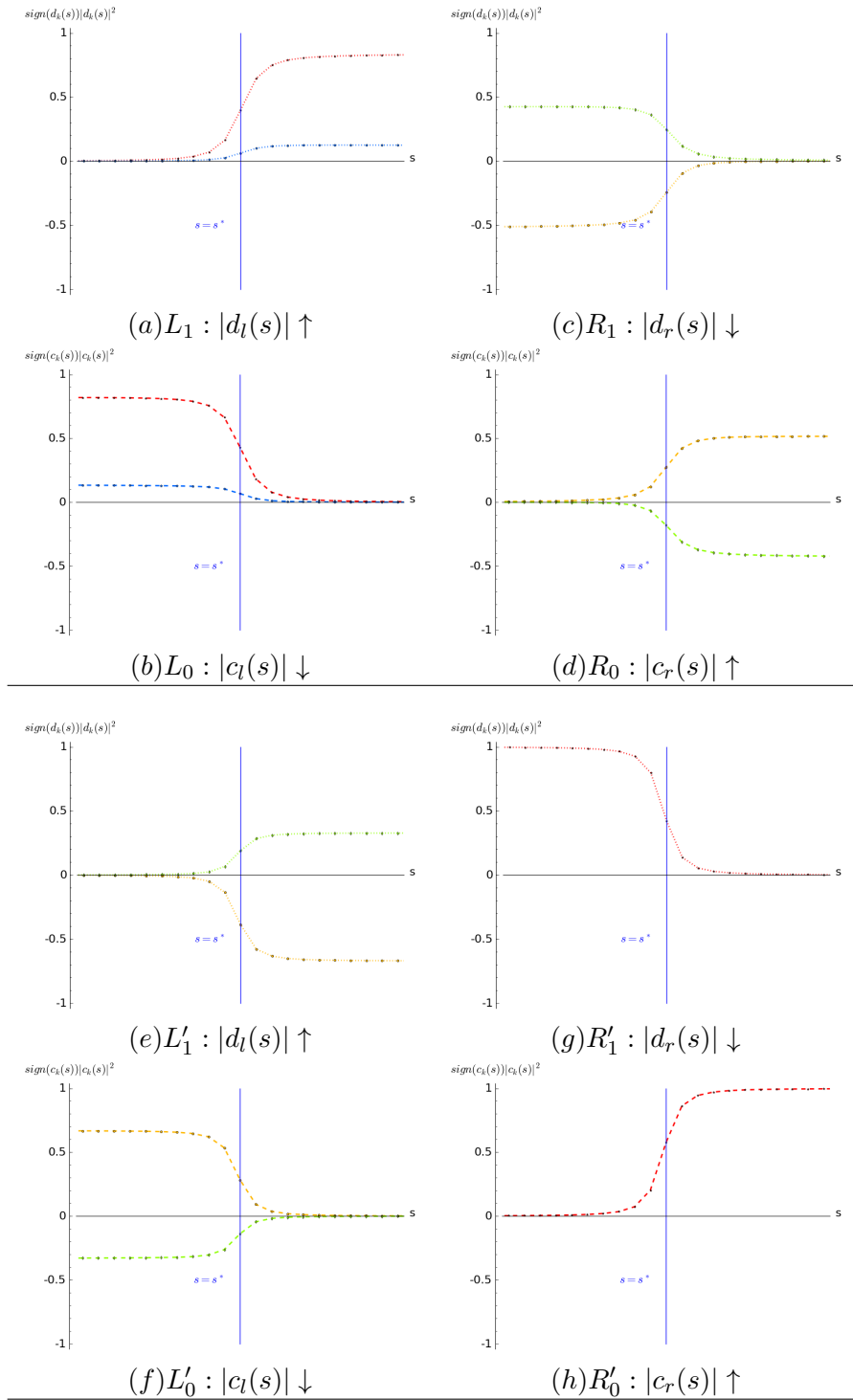


Figure 3: (Above)  $L_1$  in (a) and  $L_0$  in (b) in the same sign:  $\text{sgn}(c_l)\text{sgn}(d_l) = +1 \forall l \in L$ ;  $R_1$  in (c) and  $R_0$  in (d) in the different sign:  $\text{sgn}(c_r)\text{sgn}(d_r) = -1 \forall r \in R$ . (Below)  $L'_1$  in (e) and  $L'_0$  in (f) in the different sign;  $R'_1$  in (g) and  $R'_0$  in (h) in the same sign. These are examples from a bridged double-AC:  $(L, R)$ -ANTI-CROSSING and  $(L', R')$ -ANTI-CROSSING where  $R = L'$  is the common arm of the opposite sign which is a necessary condition for a bridged double-AC to be formed.

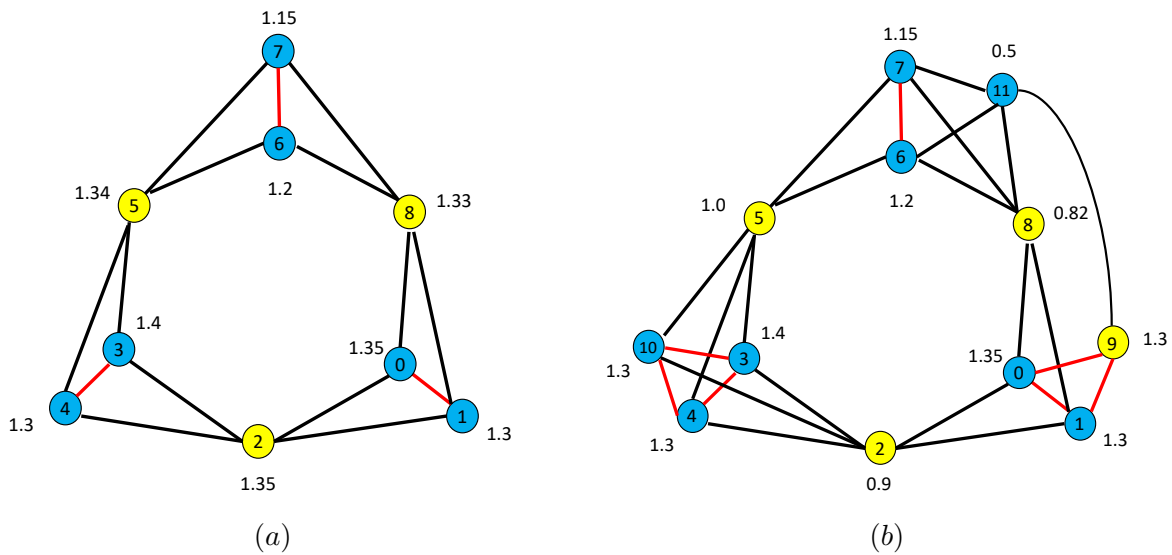


Figure 4: (a) An MIS problem graph  $G$  with 9 weighted vertices. The global minimum corresponds to the maximum independent set  $\{2, 5, 8\}$  (in yellow) with total weight of 4.02.  $G$  has 8 local minima,  $L = \{\{v_1, v_2, v_3\} : v_1 \in \{0, 1\}, v_2 \in \{3, 4\}, v_3 \in \{6, 7\}\}$ , with weights ranging from 3.70 to 3.95. The local-minima subgraph  $G|_L$  consists of 3 disjoint cliques (edges in red) :  $\{\{0, 1\}, \{3, 4\}, \{6, 7\}\}$ . This graph can be scaled to a graph of  $3n$  vertices, where the global minimum consists of  $n$  yellow vertices, while there are  $2^n$  local minima formed by  $n$  independent-cliques. (b) An MIS graph  $G'$  with 12 weighted vertices (with 3 extra vertices from  $G$  in (a)). The global minimum is  $\{2, 5, 8, 9\}$  (in yellow). There are three independent-cliques that form the local minima,  $L = \{\{v_1, v_2, v_3\} : v_1 \in \{0, 1, 9\}, v_2 \in \{3, 4, 10\}, v_3 \in \{6, 7\}\}$ . The edges in  $G'|_L$  are in red.

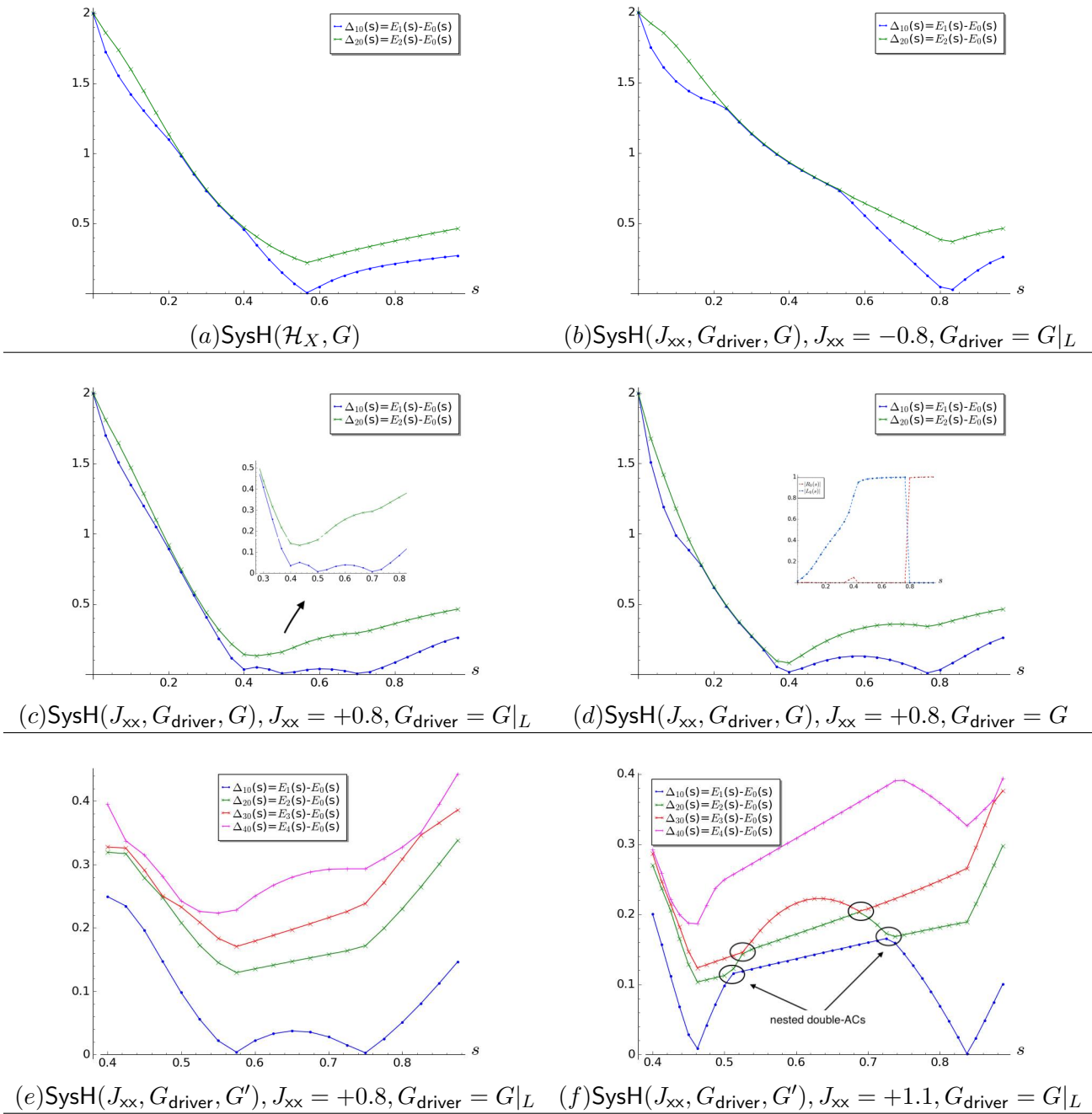


Figure 5: The *gap-spectrum* comparison of  $\text{SysH}(\mathcal{H}_X, G)$  with  $\text{SysH}(J_{xx}, G_{\text{driver}}, G)$  for the weighted graph  $G$  shown in Figure 4(a). There are one local minimum in the gap-spectrum for the stoquastic Hamiltonian in (a) and (b). There are three local minima in the gap-spectrum of the proper non-stoquastic Hamiltonian, where  $G_{\text{driver}} = G|_L$ , in (c). The last two local minima in (c) correspond to two bridged anti-crossings (a double-AC) with a large second-level gap (in green). In (d), where  $G_{\text{driver}} = G$ , there is no longer a double-AC, but one AC (the first minimum corresponds to a non-AC local minimum). In (e) and (f), the problem graph is  $G'$  in Figure 4(b). There is a double-AC with a large second-level gap for  $J_{xx} = +0.8$  in (e); there are two nested double-ACs when  $J_{xx} = +1.1$  in (f), with a large gap from the 4th-level (in magenta).



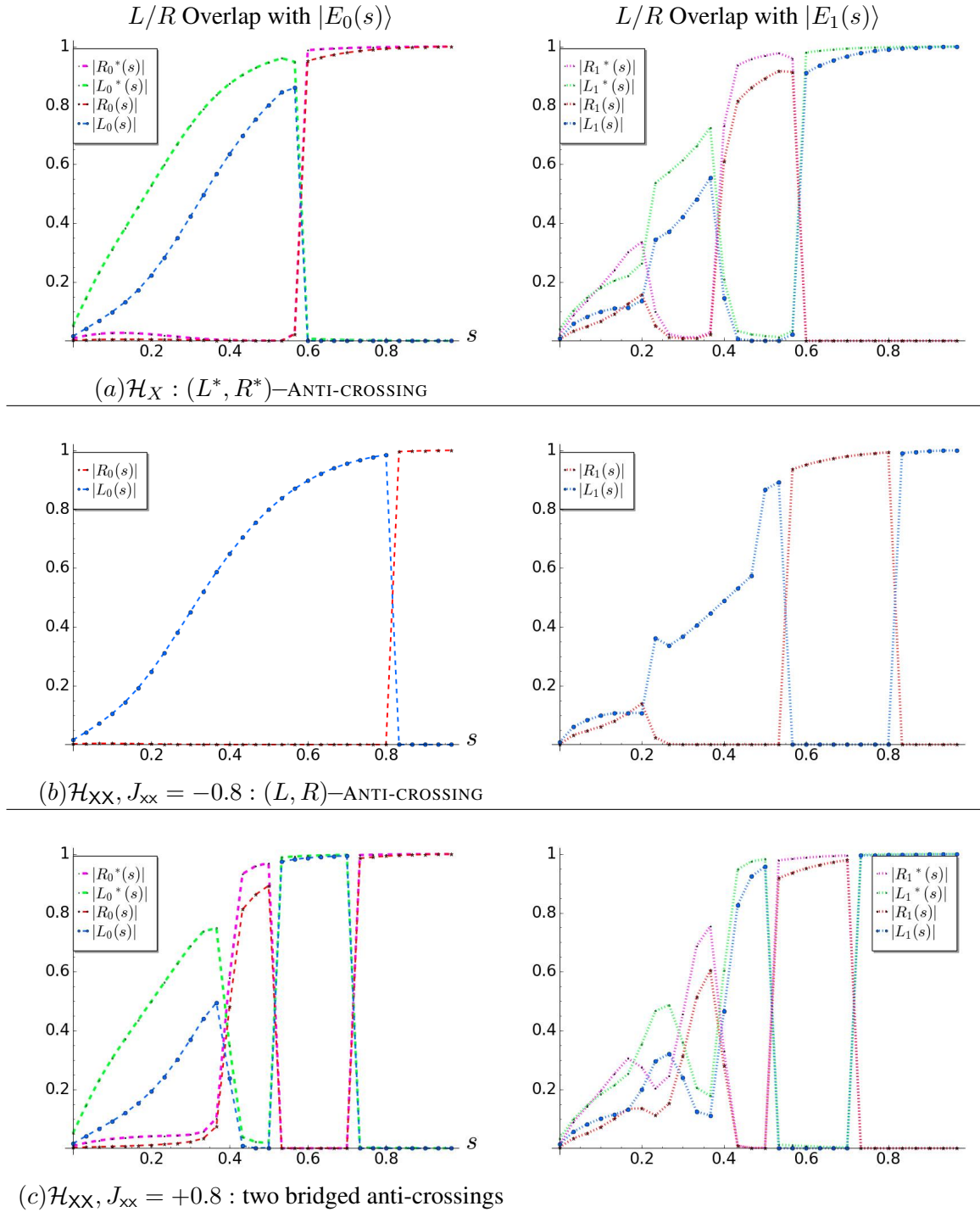
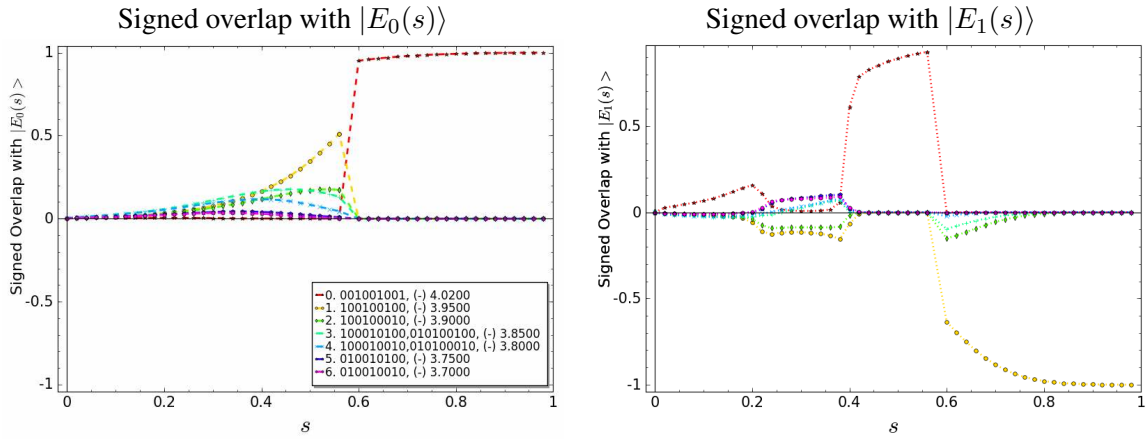
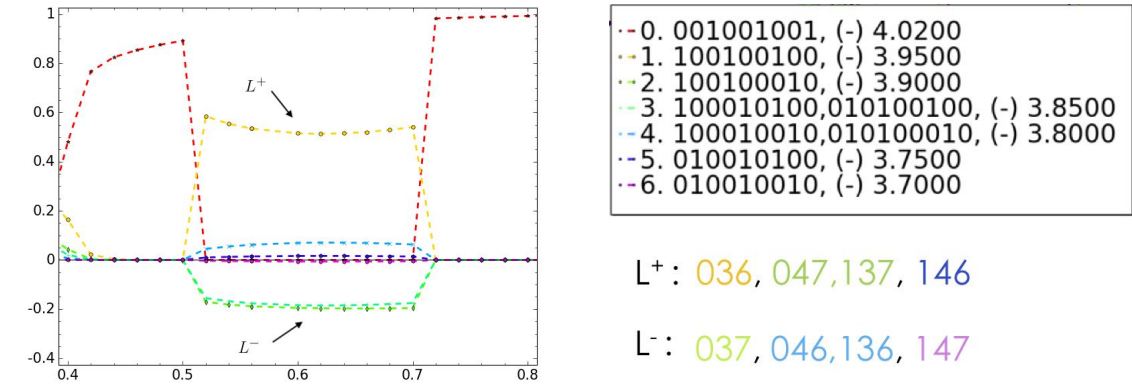
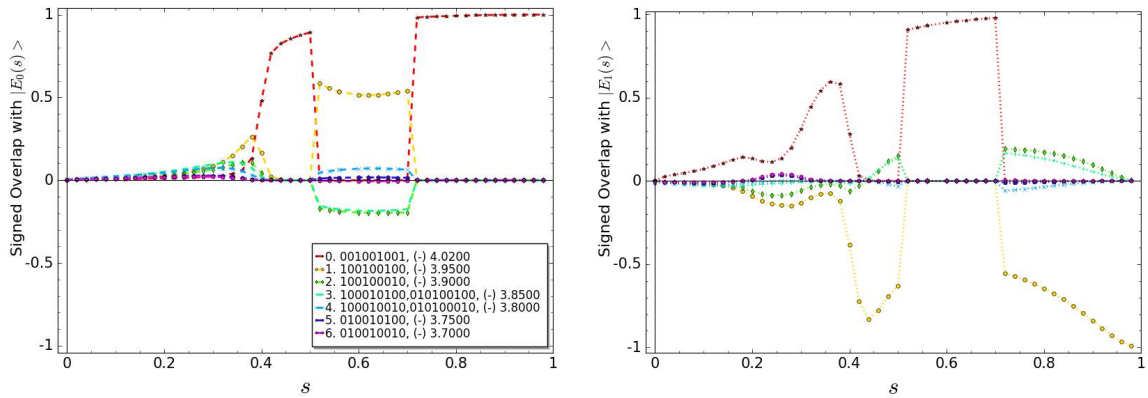


Figure 6: The “AC-signature” comparison of  $\text{SysH}(\mathcal{H}_X, G)$  with  $\text{SysH}(J_{xx}, G_{\text{driver}}, G)$  for the weighted graph  $G$  in Figure 4(a). The L/R overlaps with  $|E_0(s)\rangle$  are shown in left, and with  $|E_1(s)\rangle$  are shown in right, where  $L^* = L \cup \text{nbr}_{H_D}(L)$ ,  $R^* = R \cup \text{nbr}_{H_D}(R)$ . In both (b) and (c),  $G_{\text{driver}} = G|_L$ . In (c), there is a double-AC : (1st AC)  $(R^*, L)$ —ANTI-CROSSING at  $\sim 0.5$  and (2nd AC)  $(L, R)$ —ANTI-CROSSING at  $\sim 0.7$ .

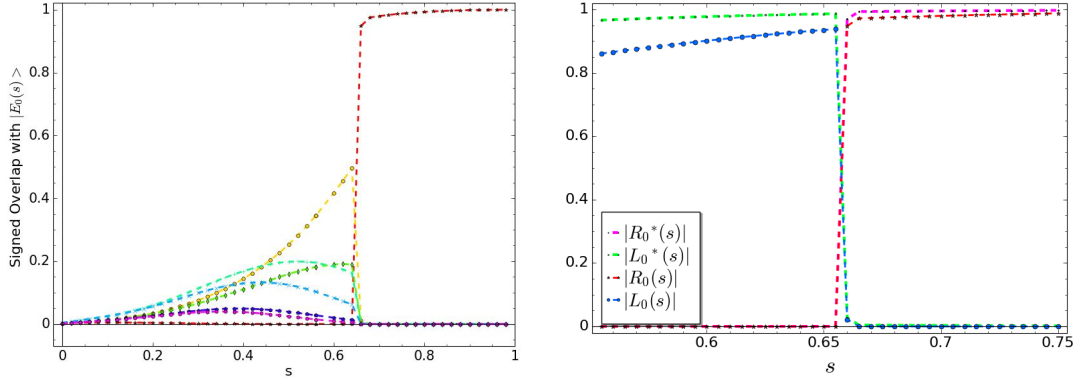


(a)  $\text{SysH}(\mathcal{H}_X, G) : (L, R)$ —ANTI-CROSSING

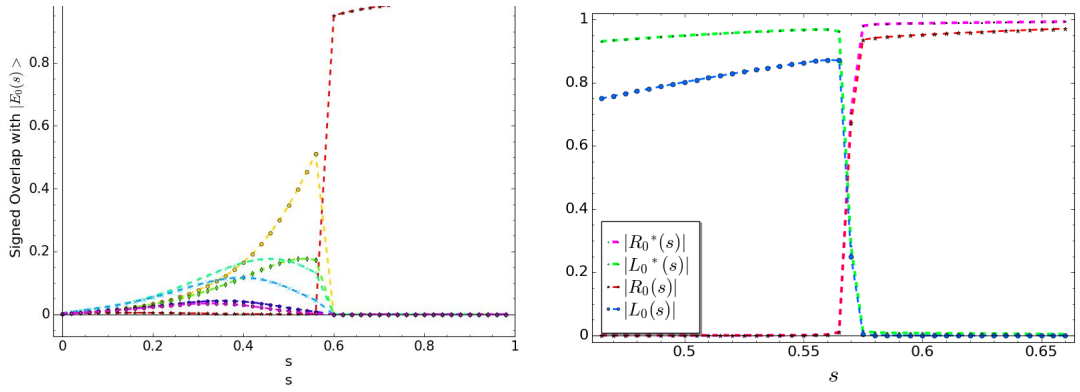


(b)  $J_{xx} = +0.8$  :  $L$  is splitted into  $L^+$  and  $L^-$

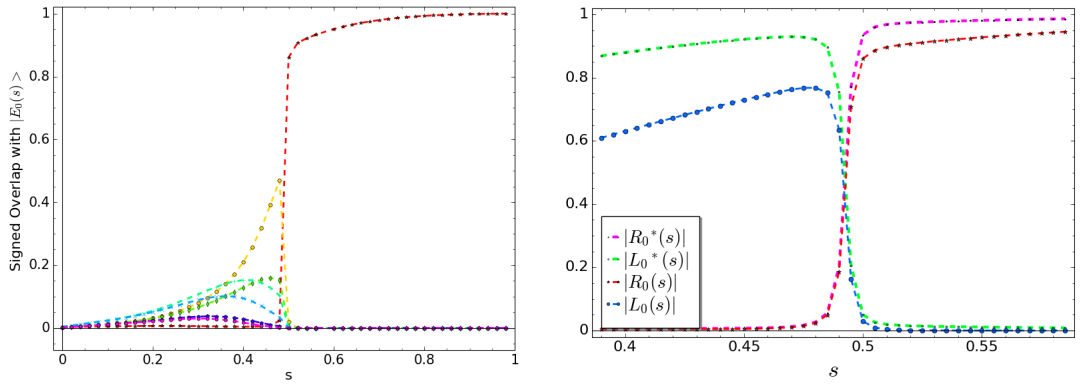
Figure 7: The *signed-overlap* comparison of  $\text{SysH}(\mathcal{H}_X, G)$  with  $\text{SysH}(J_{xx}, G_{\text{driver}}, G)$  for the weighted graph  $G$  in Figure 4(a). Signed Overlap of the seven lowest energy levels with  $|E_0(s)\rangle$  (shown in left) and with  $|E_1(s)\rangle$  (shown in right). In (b),  $G_{\text{driver}} = G|_L$ .  $L$  is split into  $L^+$  and  $L^-$ . There is exactly one XX-coupler between each state in  $L^+$  and  $L^-$ . There is either zero or more than one XX-coupler within  $L^+$  (or  $L^-$ ).



(a)  $J_{xx} = -0.3 : \Delta = 2.15e - 4, s^* = 0.6596$



(b)  $J_{xx} = 0 : \Delta = 1.58e - 3, s^* = 0.5696$



(c)  $J_{xx} = +0.3 : \Delta = 7.00e - 3, s^* = 0.4928$

Figure 8: Comparison of the overlaps of the lowest seven problem states (left) and L/R overlaps (right) with  $|E_0(s)\rangle$  of  $\text{SysH}(J_{xx}, G_{\text{driver}}, G)$ , for  $J_{xx} = -0.3, 0, +0.3$ . As  $J_{xx}$  increases (within eventually stoquastic region), the anti-crossing point  $s_x$  shifts to the right, the anti-crossing width  $\delta$  increases,  $|L_0(s_x^-)|$  decreases, resulting in the increase of the AC–Gap size.

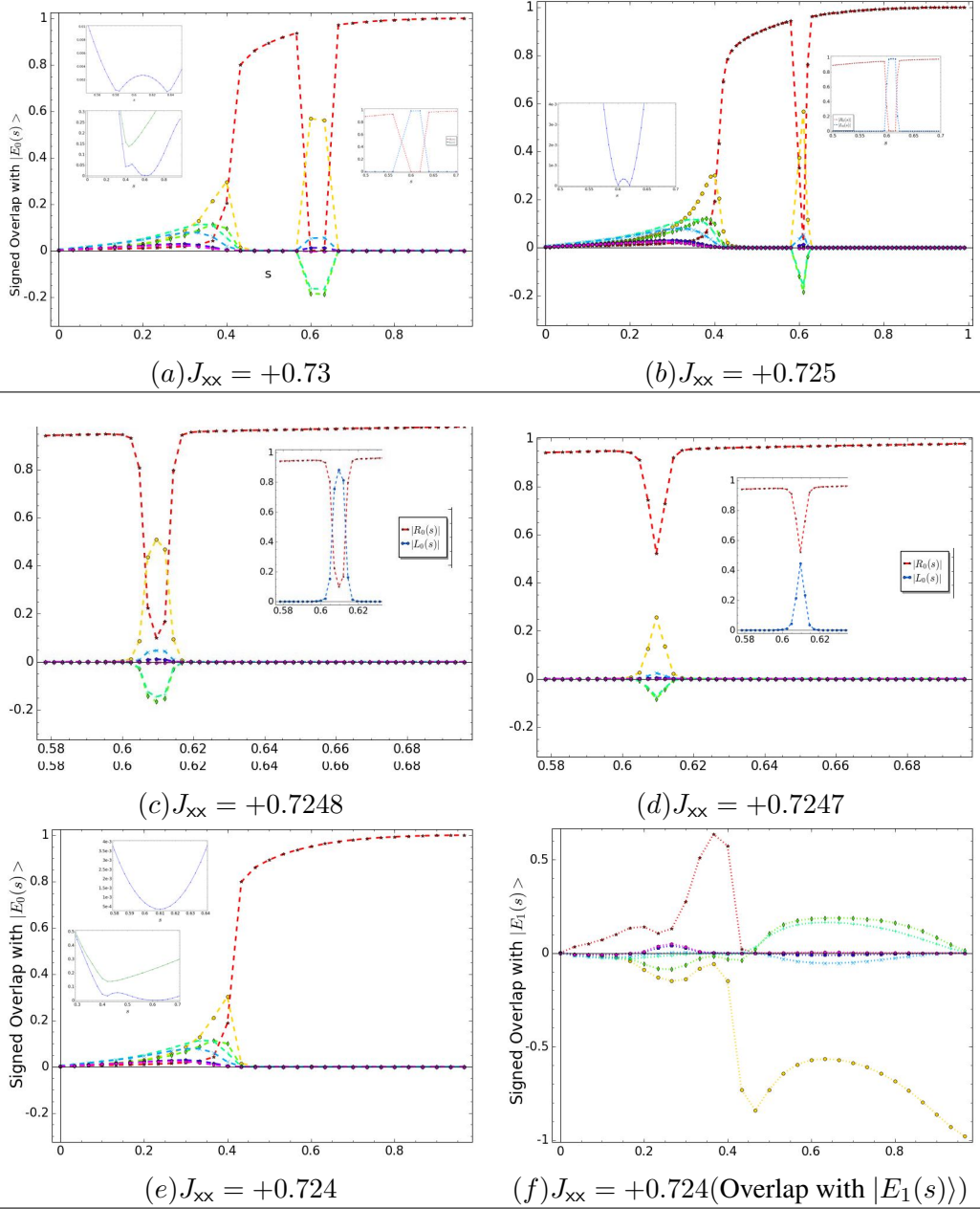
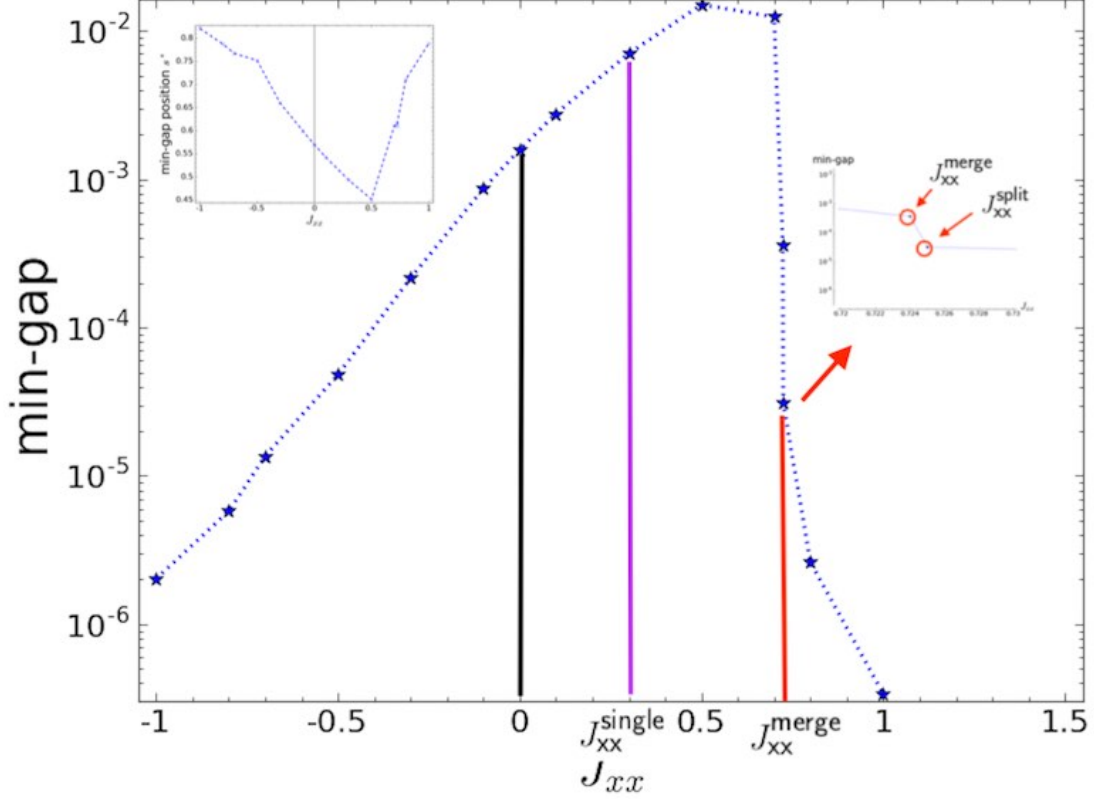
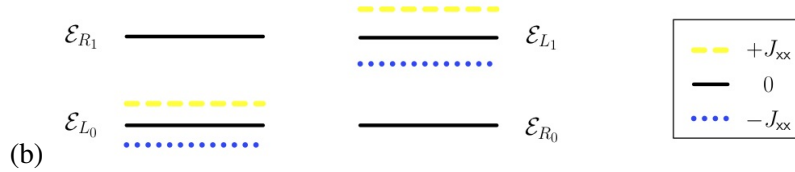


Figure 9: Evolution of the double-AC in SysH( $J_{xx}, G_{\text{driver}}, G$ ) for  $J_{xx} \in [J_{xx}^{\text{merge}}, J_{xx}^{\text{double}}]$ . As  $J_{xx}$  decreases from  $J_{xx}^{\text{double}}$ , the bridge between the two anti-crossings shrinks, as shown by comparing the results in (a) and (b). As  $J_{xx}^{\text{split}} (\approx 0.725)$  approaches  $J_{xx}^{\text{merge}} (\approx 0.724)$ , as  $s$  near the splitting point ( $s_c$ ),  $|L_0(s)|$  decreases while  $|R_0(s)|$ , as shown in (c) and (d). Eventually  $|L_0(s_c)| \approx 0$  ( $|L_1(s_c)| \approx 1$  in (e) and (f)), there is no longer an AC (as one can see from the signed overlaps in (e) and (f)); the min-gap is a non-AC local minimum in the gap spectrum. Here we see that when two ACs are merged, the ground state actually changes continuously and rapidly by “exchanging” with the first excited state not by an anti-crossing mechanism but by merging of two bridged anti-crossings.



(a)



(b)

Figure 10: (a) Min-gap  $\Delta$  vs XX-coupler strength  $J_{xx}$  of  $\text{SysH}(J_{xx}, G_{\text{driver}}, G)$  for the weighted graph  $G$  in Figure 4(a).  $J_{xx}^{\text{merge}} \approx 0.724$ ,  $J_{xx}^{\text{split}} \approx 0.725$ .  $J_{xx}^{\text{single}} \approx 0.3$ . For  $J_{xx} \in (0, J_{xx}^{\text{single}}]$ ,  $\Delta(J_{xx}) > \Delta(0) > \Delta(-J_{xx})$  (de-signed is greater); for  $J_{xx} > J_{xx}^{\text{merge}}$ ,  $\Delta(J_{xx}) < \Delta(-J_{xx})$  (de-signed is smaller). In this example, for  $J_{xx} \in (J_{xx}^{\text{single}}, J_{xx}^{\text{merge}}]$ ,  $\Delta(J_{xx}) > \Delta(-J_{xx})$  (de-signed is greater) but this is in general unknown as we do not know how small is the non-AC gap near  $J_{xx}^{\text{merge}}$ . For  $J_{xx} \in (0.3, 0.5]$ , the min-gap is a weak-AC gap. (b) For a small  $J_{xx}$ ,  $\mathcal{E}_{L_0}(-J_{xx}) < \mathcal{E}_{L_0}(0) < \mathcal{E}_{L_0}(+J_{xx})$  and  $\mathcal{E}_{L_1}(-J_{xx}) < \mathcal{E}_{L_1}(0) < \mathcal{E}_{L_1}(+J_{xx})$ ; while  $\mathcal{E}_{R_0}$  and  $\mathcal{E}_{R_1}$  stay the same because the XX-couplers in the driver graph affect  $L$  only. Also,  $\mathcal{E}_{L_1}(-J_{xx}) - \mathcal{E}_{L_0}(-J_{xx}) = \mathcal{E}_{L_1}(+J_{xx}) - \mathcal{E}_{L_0}(+J_{xx})$  (c.f. Figure 1 in [17]). Both the anti-crossing point  $s_x$  and the width  $\delta$  get shifted, result in either strengthened-AC ( $-J_{xx}$ ) or weakened-AC ( $+J_{xx}$ ) and  $\text{AC-Gap}(-J_{xx}) < \text{AC-Gap}(0) < \text{AC-Gap}(+J_{xx})$ .

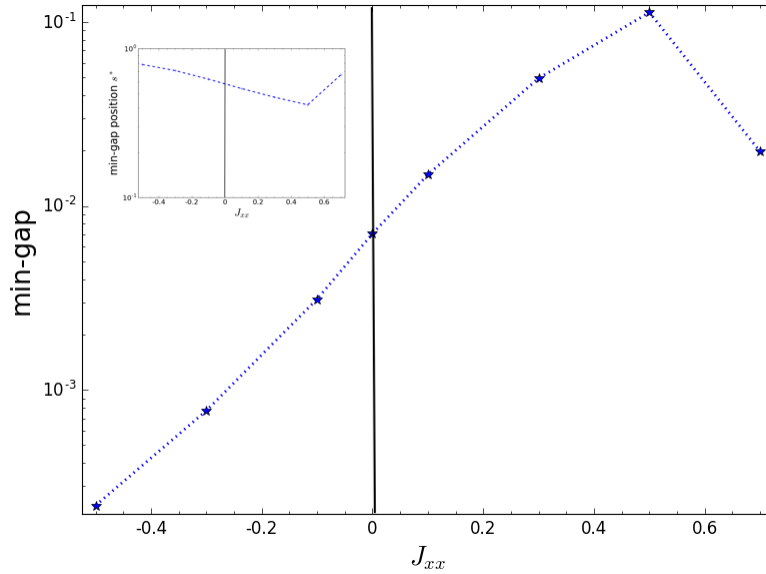


Figure 11: Min-gap  $\Delta$  vs XX-coupler strength  $J_{xx}$  of  $\text{SysH}(J_{xx}, G_{\text{driver}}, G')$  for the weighted graph  $G'$  in Figure 4(b). For  $J_{xx} \in (0, 0.5]$ ,  $\Delta(J_{xx}) > \Delta(0) > \Delta(-J_{xx})$  (de-signed is greater). A counter-example to [17].

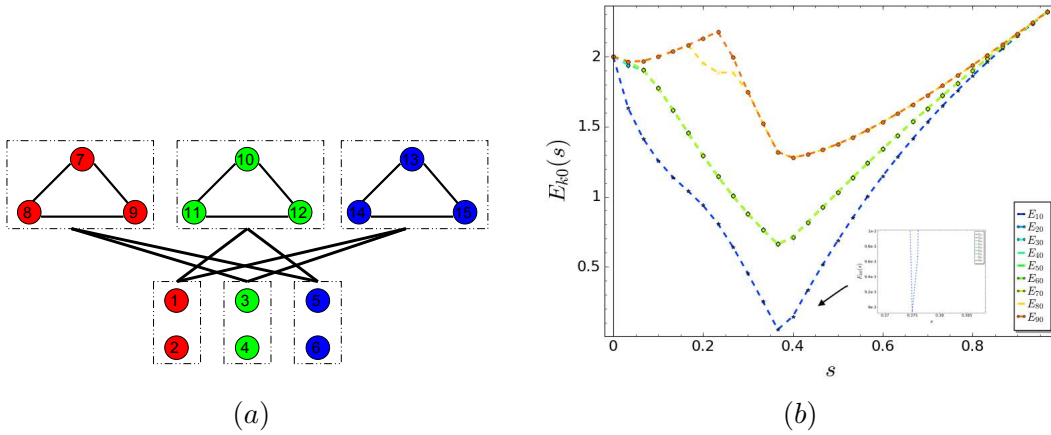
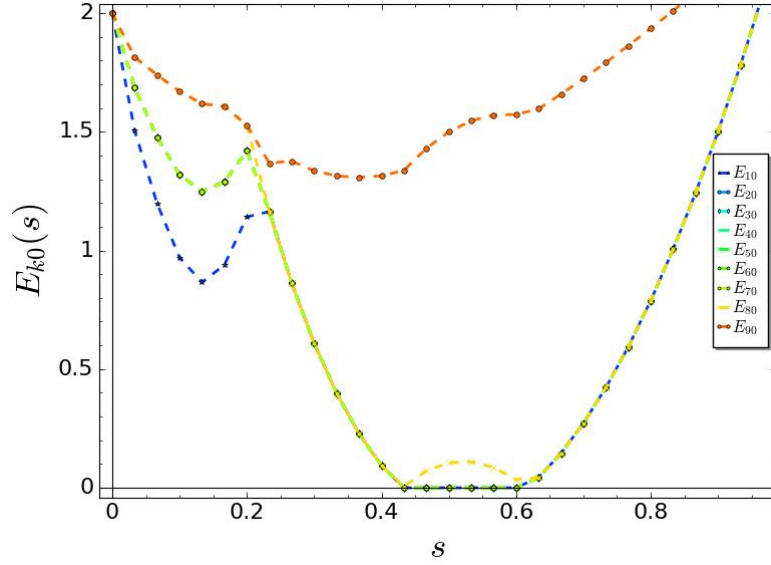
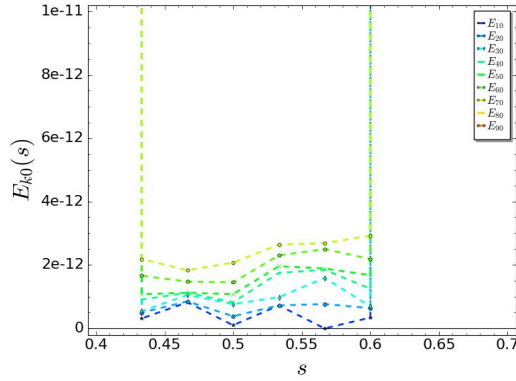


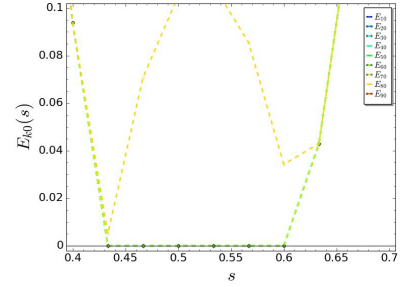
Figure 12: (a) The 15-qubit graph  $G_{rm}$  from [10]. The vertices 1..6 have a weight  $W_G$  and the vertices 7..15 (in three triangles) are weighted  $W_L$ . For  $W_L < 2W_G$ , the first six vertices make the global minimum (MWIS), while every combination of 3 vertices each from one triangle is a smaller independent set, altogether making 27 degenerate local minima. (b)  $\text{SysH}(\mathcal{H}_X, G_{rm})$  has an anti-crossing with a small gap ( $8e - 3$ ) at  $s_x = 0.375$ .



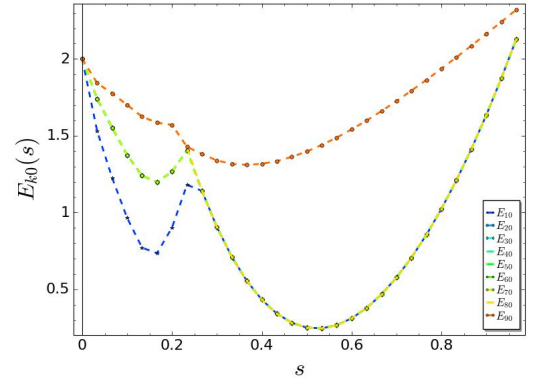
(a)  $\text{SysH}(J_{xx}, G_{\text{driver}}, G_{rm}), J_{xx} = 2.5$



(a1)  $s \in [s_1, s_2] : E_{k0}(s) < 3e - 12$



(a2)  $s \in [s_1, s_2] : E_{80}(s) > 0.01$



(b)  $\text{SysH}(J_{xx}, G_{\text{driver}}, G_{rm}), J_{xx} = 2$

Figure 13: The gap-spectrum for  $\text{SysH}(J_{xx}, G_{\text{driver}}, G_{rm})$  where the weighted graph  $G_{rm}$  shown in Figure 12, with  $W_L = 1.8$ ,  $W_G = 1$ ,  $G_{\text{driver}}$  consists of the three triangles, (a)  $J_{xx} = 2.5$ ; (b)  $J_{xx} = 2.0$ . (a) There is a double *multi-level* anti-crossing at  $s_1 = 0.43$  and  $s_2 = 0.6$ . For  $s \in [s_1, s_2]$ ,  $E_{k0}(s) < 3e - 12$  (shown in (a1)) for  $k = 1..7$ , and  $E_{80}(s) > 0.01$  (shown in (a2)). The lowest 7 excited states ( $|E_1\rangle \dots |E_7\rangle$ ) form a narrow band (as if it is a pseudo-degenerate state). As with the diabatic cascade [8], the system can diabatically transition to  $|E_7(s)\rangle$  at  $s_1$ , and then through another diabatic cascade transition back to  $|E_0(s)\rangle$  at  $s_2$ , when annealing time is short. One can further verify if indeed DQA-GS can be successfully applied to this example through HOQST [33]. Remark: if one perturbs the vertex weights so as to break the  $3^3$ -fold degeneracy, one would obtain a sequence of nested double-ACs for some  $J_{xx}$ . (b) There is no AC with  $\text{min-gap} = 0.244$  at  $0.523$ . For  $J_{xx} \in [0.5, 2.2]$ , there is no AC and the  $\text{min-gap}$  is large.